

**OPTIMIZATION OF  $\text{Cu}_2\text{O}$   
PHOTOACTIVE LAYER FOR  
SUSTAINABLE INTEGRATION ON  
ALL OXIDE SOLAR CELL FOR  
SELF-POWERED SMART WINDOWS**



**By**

**Ramsha Durrani**

**Talha Ahmed**

**Amna Malik**

**School of Chemical and Materials Engineering  
National University of Sciences and Technology**

**2024**

# **OPTIMIZATION OF $\text{Cu}_2\text{O}$ PHOTOACTIVE LAYER FOR SUSTAINABLE INTEGRATION ON ALL OXIDE SOLAR CELL FOR SELF-POWERED SMART WINDOWS**



**Leader - 324997 Ramsha Durrani**

**Member-1 - 339813 Talha Ahmed**

**Member-2 - 343222 Amna Malik**

**A THESIS**

Submitted to

National University of Sciences and Technology

in partial fulfilment of the requirements for the degree of

**B.E. METALLURGY AND MATERIALS ENGINEERING**

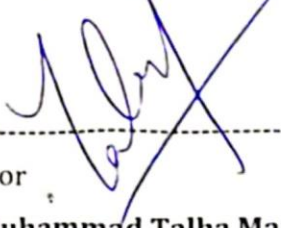
**School of Chemical and Materials Engineering (SCME)**

**National University of Sciences and Technology (NUST)**

**June 2024**

## CERTIFICATE

This is to certify that work in this thesis has been completed by **Ms. Ramsha Durrani, Mr. Talha Ahmed** and **Ms. Anna Malik** under the supervision of **Dr. Muhammad Talha Masood** and **Dr. Malik Adeel Umar** at the school of Chemical and Materials Engineering (SCME), National University of Science and Technology, H-12, Islamabad, Pakistan.



-----  
Advisor

**Dr. Muhammad Talha Masood**

Department of Materials Engineering  
School of Chemical and Materials  
Engineering  
National University of Sciences and  
Technology

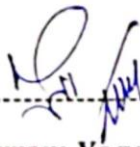


-----  
Co-Advisor

**Dr. Malik Adeel Umar**

Department of Materials Engineering  
School of Chemical and Materials  
Engineering  
National University of Sciences and  
Technology

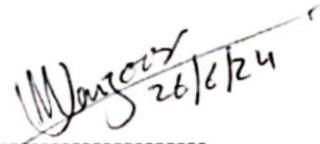
Submitted Through:



HOD-----

**Dr. Khurram Yaqoob**

Department of Materials Engineering  
School of Chemical and Materials  
Engineering  
National University of Sciences and  
Technology



Principal-----

**Dr. Umair Manzoor**

Department of Materials Engineering  
School of Chemical and Materials  
Engineering  
National University of Sciences and  
Technology

## **DEDICATION**

This thesis stands as a testament to the steadfast support and contributions of our parents, teachers, and friends. We are deeply grateful for your faith in us and the crucial roles you have played in making this achievement a reality. This work is also dedicated to that inspired junior who is reading this, curious to know more about the future works on Solar Cells.

## DECLARATION

We, **Ramsha Durrani, Talha Ahmed** and **Amna Malik** declare that this thesis titled "**Optimization of Cu<sub>2</sub>O Photoactive layer for Sustainable Integration on All Oxide Solar Cell for Self-powered Smart Windows**" is our original work completed as a prerequisite for the fulfilments of our bachelor's degree in Metallurgy and Materials Engineering. Under the supervision of **Dr. Muhammad Talha Masood**, we conducted the research, analyzed the data, and formulated the conclusions with no plagiarism. All sources used have been appropriately cited, and ethical guidelines have been followed. This work is submitted to the **Department of Materials Engineering SCME** as a requirement for the completion of our bachelor's degree program.

## ACKNOWLEDGEMENTS

Firstly, we would like to Allah Almighty to enable us to make this project possible, indeed, there is nothing possible without his guidance. We wish to extend our deepest gratitude to our project supervisor, **Dr. Muhammad Talha Masood**, for his exceptional guidance, unwavering support, and invaluable insights throughout this project. His expertise, patience, and steadfast commitment to our academic growth have been pivotal in the success of this endeavor.

We also sincerely thank **Dr. Sofia Javed** and **Dr. Malik Adeel Umar** for their assistance in interpreting the characterization data. We are grateful to **Dr. Sofia Javed** for allowing us to use her lab, as well as to all the senior colleagues and lab assistants who helped us during the project. Their informative conversations, support with identifying problems and helpful criticism helped us get past experimental obstacles and produce significant outcomes.

We would like to sincerely thank each and every faculty member of SCME Materials Department for their invaluable contributions to our education. Their commitment to mentoring and intellectual engagement has deepened our knowledge and expanded our horizons in this area.

Finally, we thank SCME NUST for its resources and cooperation. The academic community, the library resources and the facilities were all quite helpful in helping us finish our final year project.

## ABSTRACT

Smart windows are innovative window systems that are essential for sustainable building design because they can dynamically modify their transparency and boost energy efficiency by optimizing natural light, lowering the need for artificial lighting, and minimizing the strain on heating and cooling systems. An individual smart window requires very little electrical power to operate; but, if many of these windows are incorporated into a building, the power requirement may increase dramatically, resulting in higher costs for building maintenance. In order to incorporate All-Oxides Solar Cells (AOSCs) on smart windows for self-sustainability, we therefore intend to explore the prospect of investigating AOSCs as a renewable and continuous source of electricity during this research project. The foundation of AOSCs is semiconducting, economically viable solution-processable metal oxides. In contrast to perovskite solar cells, which need an inert atmosphere to prepare the photoactive layer, the production of these solar cells can be done in ambient settings. Silicon-based solar cells, on the other hand, are costly and opaque. Since AOSCs are transparent and stable against environmental factors, they may be the best choice to incorporate into smart windows for their self-sustainability. Our goal in this work is to optimize the  $\text{Cu}_2\text{O}$  thin film for  $\text{Cu}_2\text{O}/\text{TiO}_2$  planar heterojunction AOSC by using it as a photoactive p-type semiconductor. Under normal device testing protocols, the optimized  $\text{Cu}_2\text{O}$  will be integrated into the ultimate photovoltaic device and tested against achieved power output. Based on the obtained power output, the experimental demonstration will be proposed to power a unit area of a given smart window.

# TABLE OF CONTENT

CHAPTER 1.....	1
1. INTRODUCTION.....	1
1.1 Background.....	1
1.2 Problem Statement.....	2
1.3 Problem Description.....	2
1.4 Scope.....	2
1.5 Purpose.....	3
1.6 Project Objectives.....	4
CHAPTER 2.....	7
2. LITERATURE REVIEW.....	7
2.1 Phenomenon of Photovoltaics for Energy Conversion.....	7
2.2 Cu <sub>2</sub> O as a p-type layer.....	8
2.3 Deposition technique of Cu <sub>2</sub> O film.....	9
2.4 Heterojunction Solar cell.....	10
2.5 Properties of Cu <sub>2</sub> O as thin films.....	10
2.6 Electrical properties of Cu <sub>2</sub> O.....	11
CHAPTER 3.....	13
3. DEVICE ARCHITECTURE.....	13
3.1 Device Structure.....	14
CHAPTER 4.....	15
4. METHODOLOGY.....	15
4.1 Surface Treatment.....	15
4.2 Fabrication Of Photoactive Layers.....	16
4.2.1 Fabrication and deposition of Cu <sub>2</sub> O film on Soda lime glass and FTO Glass using SILAR method.....	16
4.2.2 Fabrication and Deposition of TiO <sub>2</sub> using Spin Coating for TiO <sub>2</sub> (TTIP) based acidic solution.....	18
4.2.3 Calcination of TiO <sub>2</sub> and Cu <sub>2</sub> O for Phase Transformation.....	20
4.2.4 Thermal Evaporation for back metal contacts.....	20



4.2.5	Solar Simulation for I-V Curves .....	21
CHAPTER 5.....		22
5.	TESTING AND RESULTS.....	22
5.1	Characterization of Titania layer (N-Type).....	22
5.1.1	Scanning Electron Microscopy (SEM).....	22
5.1.3	UV-VIS Spectroscopy.....	25
5.1.4	RAMAN Spectroscopy.....	27
5.2	Characterization of Copper 1 Oxide layer (P-Type).....	29
5.2.1	Scanning Electron Microscopy (SEM).....	29
5.2.2	Energy dispersive X-ray spectroscopy.....	35
5.2.3	UV-Vis Spectroscopy.....	44
CHAPTER 6.....		51
SOLAR SIMULATION USING I-V CURVES.....		51
6.1	Light.....	51
6.2	Dark.....	52
CHAPTER 7.....		54
INTEGRATION OF AOSCs ON SMART WINDOW.....		54
CONCLUSION .....		55
9.	REFERENCES .....	56
APPENDIX .....		58
What does the future hold?.....		58
Integration of AOSCs on Perovskite solar cell.....		58

## LIST OF FIGURES

Figure 1 Illustrating the electron hole pair distribution. ....	7
Figure 2 The device model of the heterojunction system.....	14
Figure 3 SILAR Method for deposition of Copper (I) Oxide layer .....	18
Figure 4 Method of Deposition of Titania.....	20
Figure 5 SEM images for magnification A) x5000 B) x15000 C) x30000 D) x50000	22
Figure 6 Elemental composition for Titania.....	24
Figure 7 EDX results for Titania.....	24
Figure 8 Absorbance vs Wavelength graph for Titania .....	25
Figure 9 RAMAN spectroscopy for Titania .....	27
Figure 10 SEM Images on magnification A) x5000 B) x20000 C) x10000 D) x30000 .....	29
Figure 11 SEM Images on magnification A) x5000 B) x10000 C) x20000 D) x30000 .....	30
Figure 12 SEM Images for magnification A) x5000 B) x30000 C) x10000 D) x20000 .....	32
Figure 13 SEM Images for magnification A) x5000 B) x20000 C) x10000 D) x30000 .....	34
Figure 14 Elemental composition of Copper (I) Oxide at 100 Non-Calcinated.....	35
Figure 15 EDX Results for Copper (I) Oxide at 100 Non-Calcinated.....	36
Figure 16 Elemental Composition of Copper (I) oxide at 100 Calcinated .....	38
Figure 17 EDX Results for Copper(I)Oxide at 100 Calcinated.....	38
Figure 18 Elemental Composition of Copper (I) Oxide at 200 Non-Calcinated.....	40
Figure 19 EDX Results for Copper (I) Oxide at 200 Non-Calcinated.....	40
Figure 20 Elemental composition of Copper (I) Oxide at 200 Calcinated.....	42
Figure 21 EDX Results for Copper (I) Oxide at 200 Calcinated.....	42
Figure 22 Absorbance vs Wavelength graph for Copper (I) Oxide at different Cycles .....	44
Figure 23 Absorbance vs Wavelength graph for Calcinated and Non-Calcinated Copper (I) Oxide .....	45

Figure 24 Tauc Plot showing Energy Gap values at different cycles .....	46
Figure 25 Tauc Plot showing Energy Gap values of Calcinated and Non-Calcinated Samples of Copper(I)Oxide .....	48
Figure 26 RAMAN Spectroscopy of Calcinated and Non-Calcinated Copper(I)Oxide at A)200 Cycles and B)100 Cycles .....	49
Figure 27 Solar Simulation in Light .....	51
Figure 28 Solar Simulation in Dark.....	52

## ABBREVIATIONS

- PV-Photovoltaic
- BIPV- Building Integrated Photovoltaic
- AOSC- All oxide Solar Cells
- c-Si PV-crystalline silicon photovoltaic
- PDLC- Polymer Dispersed Liquid Crystal
- ETL- Electron Transport Layer
- Cu<sub>2</sub>O- Cuprous Oxide
- TiO<sub>2</sub>- Titania
- FTO- Fluorine-Doped Tin Oxide
- TCO- Transparent Conducting Oxide
- ITO-Indium Tin Oxide
- Voc- Open Circuit Voltage
- SILAR- Successive Ion Layer Adsorption and Reaction
- SEM- Scanning Electron Microscopy
- RAMAN- RAMAN Spectroscopy (Named after Indian Physicist Raman)
- UV-Vis- Ultra-Violet Visible Spectroscopy
- XRD- X-Ray Diffraction
- EDX- Energy Dispersive X-Ray Spectroscopy

# CHAPTER 1

## 1. INTRODUCTION

An important technical development for energy efficiency and sustainable living is the incorporation of transparent solar cells into smart windows. This cutting-edge combination of smart window systems and transparent solar technology is transforming how windows support the energy requirements and self-sustainability of a building. By acting as energy producers and efficiently collecting and using solar electricity throughout the day, smart windows with transparent solar cells help to maximize energy efficiency. This method reduces dependency on conventional power sources, which lowers utility costs and lowers carbon emissions. As a result, it aligns with the global trend of using more renewable energy.

All Oxide Solar Cells (AOSCs) are transparent, flexible, and efficient solar cells that represent a revolutionary replacement for conventional silicon-based solar cells. These materials are becoming more popular in AOSCs and are perfect for intelligent window systems. This introduction highlights the potential of AOSCs in advancing sustainable energy solutions by examining their transformative powers and their use in environmentally friendly architecture and intelligent windows.

### 1.1 Background

Innovative technologies that improve energy efficiency and lower carbon footprints are being studied because of the increased need for sustainable energy solutions. Conventional building materials are being repurposed for several purposes, especially in the field of renewable energy production. A significant advancement in this field is represented by transparent solar cells, which enable the use of solar energy without sacrificing visibility or aesthetics. In order to produce self-sustaining structures, this research focuses on integrating All Oxide Solar Cells (AOSCs) into smart windows. Through the integration of photovoltaic capabilities and

transparency, AOSCs hold the potential to transform green design and make a significant contribution to a sustainable future.

## **1.2 Problem Statement**

### **SMART WINDOWS: EFFICIENT OR NOT?**

Smart Windows, when installed in large quantity for a building, **requires higher voltage supply** to alter its transparency, making it non sustainable.

## **1.3 Problem Description**

Smart windows face substantial obstacles in terms of general application, even though they have the potential to improve energy efficiency and comfort by altering their transparency based on environmental conditions. One of the most important issues is the high voltage required to alter the transparency of these windows, especially when they are placed in large quantities on BIPVs inside of buildings. Smart windows may not be as sustainable overall due to their high energy consumption, as the electricity needed to operate them can outweigh the energy savings they provide. As a result, the growing power consumption and associated costs raise concerns about the feasibility and environmental impact of large-scale smart window installations.

## **1.4 Scope**

The objective of this research is to assess and improve transparent All Oxide Solar Cells (AOSCs) integrated smart window technology. In order to ensure sustainability even in large-scale applications, it focuses on evaluating the energy-saving potential of these windows in a variety of building types and settings and creating techniques to lower their high voltage requirements. To assess AOSCs' suitability for smart windows, the project comprises a thorough investigation of their characteristics with a focus on their transparency, adaptability, and efficiency.

Additionally, it also looks at the environmental effects by examining how this innovation reduces carbon emissions and saves utility costs. To demonstrate real-world applications and validate theoretical models, prototypes will be created and put through testing. Additionally, a thorough cost-benefit analysis will be carried out to determine the financial effects and possible savings for businesses and consumers. The project aims to promote smart window recognition and viability as a sustainable solution in contemporary design by tackling these issues.

## **1.5 Purpose**

### **1. Why are smart windows important?**

The way we interact with windows and glass surfaces is being revolutionized by technologies such as Smart Glass and Smart Film. By maximizing the use of natural light, reducing heat gain, and dynamically altering tint levels, they lessen the need for artificial lighting and air conditioning. Energy savings and environmental preservation result from this. Additionally, customers can customize their privacy solution using Smart Glass and Film by just flipping a switch to adjust the glass's opacity. They safely protect interior furniture and occupants from dangerous UV rays. They are essential for thermal insulation because they minimize heat gain in warmer weather and reduce heat loss in winter months. By combining these technologies, sufficient natural light penetration is ensured, resulting in bright, well-lit areas that improve wellbeing and productivity. They also improve security measures by adding another line of defense against vandalism and break-ins. These technologies are very useful in both professional and educational contexts because they can be used as interactive whiteboards or back projection displays.

### **2. Why should solar cells be integrated with smart windows?**

- **Energy Efficiency:** Many commercial and office buildings have windows made of shiny glass. If smart windows were used across the infrastructure in place

of conventional glass windows, a substantial quantity of electricity would be needed to keep them operating.

In terms of the electricity needed to power them, the buildings might become self-sufficient if partially transparent AOSCs are combined with such smart windows.

- **Market Growth:** Research and development in this field can spur economic growth by creating new companies and employment opportunities related to the manufacture, installation, and upkeep of smart windows.
- **Cost reduction:** Our research could lead to more affordable production methods, bringing down the price of smart windows for both businesses and consumers.

### **3. Integrating AOSCs in smart windows:**

- **Using solar energy to power smart windows:** Smart windows with integrated partially transparent solar cells have the ability to collect and transform solar energy into power. In the future, this renewable energy source may contribute to the production of more sustainable energy enabling for a better tomorrow.
  - **Sustainable Smart Buildings:** The concept of smart buildings is enhanced by the integration of partially transparent solar panels with smart windows. These buildings can maximize energy efficiency by producing and managing their own energy using sophisticated control systems for building integrated Photovoltaics.
  - **Grid Support:** Buildings with integrated solar-powered smart windows have the capacity to feed any excess energy back into the grid, which helps to stabilize it and lightens the load during periods of high demand.'

## **1.6 Project Objectives**

- 1. To create transparent solar cells with high energy conversion efficiency**



Creating transparent solar cells with a high energy conversion efficiency is the goal. In order to generate enough energy and ensure sufficient transmission of visible light for natural lighting and occupant comfort, optimal transparency is necessary. By smoothly integrating renewable energy generation into building infrastructure and preserving customer happiness, achieving this goal improves sustainability.

**2. To fabricate  $\text{Cu}_2\text{O}/\text{TiO}_2$  planar heterojunction All Oxide Solar Cells (AOSC) device on top of FTO coated glass and microscopic glass substrate.**

The implementation of All Oxide Solar Cells (AOSC) devices on FTO-coated glass substrates is an important goal that will have a significant impact on sustainable energy technology. This project produces compact  $\text{TiO}_2$  layers by using an optimized spin-coating method, which guarantees effective light absorption and charge separation inside the solar cell structure. The endurance and performance of the device are further improved by selecting back-metal contacts made of aluminum or silver that are deposited using a thermal evaporator setup. This goal could revolutionize the scalability and efficiency of transparent solar technology, marking a breakthrough in the field of renewable energy research. The successful manufacture of these AOSC devices suggests that smart window systems will be widely used, which will help reduce energy consumption and the environmental effect of buildings globally.

**3. To characterize the heterojunction photoactive layer of  $\text{Cu}_2\text{O}$  and Titania using SEM, XRD, RAMAN**

Our goal is important because it has the potential to progress materials science and renewable energy technologies. Through the use of the SILAR process, we can create copper oxide ( $\text{Cu}_2\text{O}$ ) films on soda lime glass, opening up new possibilities for improving the performance and efficiency of transparent solar cells. By utilizing RAMAN, SEM, and UV-VIS spectroscopy to characterize these thin films, we may gain an understanding of their structural, morphological, and optical features that are

essential for the conversion of solar energy. By improving film thickness, the manufacturing process can be further optimized, which could lead to an increase in energy capture and total device efficiency. This discovery holds potential for the widespread deployment of transparent solar technologies in buildings and urban infrastructure, thereby aiding in the development of affordable, sustainable energy alternatives.

**4. To propose the size of this semi-transparent solar cell to power a unit area of a given PDLC smart window.**

This goal is extremely important since it seeks to ascertain the ideal size of semi-transparent solar cells needed to effectively power a smart window's unit area. Reaching this objective will allow the initiative to improve the energy efficiency of smart windows, which could result in large savings on utility and electricity bills. Moreover, the attachment of a polymer dispersed liquid crystal layer (PDLC) to the rear of the FTO glass substrate may enhance solar cell performance and yield further advantages in terms of functionality and sustainability.

2. LITERATURE REVIEW

2.1 Phenomenon of Photovoltaics for Energy Conversion

Chapter 11 - All-Oxide Solar Cells

*Theodoros Dimopoulos, Chapter 11 - All-Oxide Solar Cells, Editor(s): Monica Lira-Cantu, In Metal Oxides, The Future of Semiconductor Oxides in Next-Generation Solar Cells, Elsevier, 2018, Pages 439-480. [1]*

Heterojunction solar panels, a unique technology, combine conventional wafer-based photovoltaic (PV) technology with thin-film technology, enhancing their performance. This requires a thorough analysis of materials, structure, manufacturing, and classification, unlike conventional solar cells.

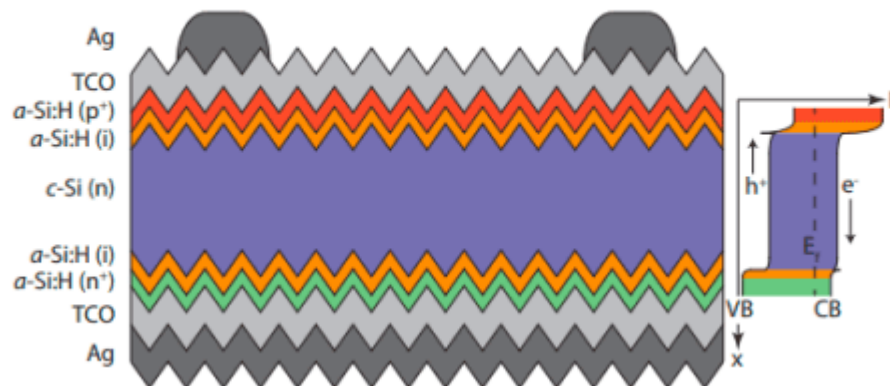


Figure 1 Illustrating the electron hole pair distribution.

Heterojunction solar panels utilize a trilayer structure, combining thin-film and standard photovoltaic technologies, to enhance absorption capabilities. The process involves connecting the load to the module terminals, as shown in the figure 1,

converting photons into electrical energy, and generating an electric current. The incident photon interacts with the P-N junction absorber, excitation of an electron, and transition to the conduction band, generating an electron-hole pair. The terminal attached to the P-doped layer serves as the recipient for the excited electron, generating an electric current that passes through the load.

Upon traversing the load, the electron returns to the rear contact of the cell, where it recombines with a hole, terminating the specific electron-hole pair. Power generation is continuous, facilitated by the module's operation. Surface recombination is a common issue in conventional crystalline silicon photovoltaic (c-Si PV) modules, limiting their overall efficiency. To prevent surface recombination, Heterojunction with Intrinsic Thin-layer (HJT) solar cells use a passivating semiconductor film composed of amorphous silicon with a larger bandgap layer. The presence of a buffer layer in the HJT cell enables controlled deceleration of charge flow, generating a high voltage potential, circumventing electron recombination before collection, enhancing the overall efficiency of the HJT cell.

## **2.2 Cu<sub>2</sub>O as a p-type layer**

### **Design Rules for Donors in Bulk-Heterojunction Solar Cells— Towards 10 % Energy-Conversion Efficiency**

*Scharber, M.C., Mühlbacher, D., Koppe, M., Denk, P., Waldauf, C., Heeger, A.J. and Brabec, C.J., 2006. Design rules for donors in bulk-heterojunction solar cells—Towards 10% energy-conversion efficiency. Advanced materials, 18(6), pp.789-794. [2]*

To increase energy conversion efficiencies, this article explains the design guidelines for donors in bulk-heterojunction solar cells. The low device efficiencies of organic solar cells have been a major roadblock to their commercialization, even though they have the potential to greatly cut the cost of photovoltaics[3]. The authors investigated the connection between the donor-acceptor mix energy and the solar cell's open-

circuit voltage ( $V_{oc}$ ). They discovered that the  $V_{oc}$  is set by the difference between the acceptor's LUMO energy level and the polymer donor's HOMO energy level. To determine the maximum efficiency of bulk-heterojunction solar cells, they used their results to draw a simple link between the donor HOMO level and the  $V_{oc}$ . The importance of maximizing the LUMO level of the donor material was also brought to light by their research[4].

### **2.3 Deposition technique of $Cu_2O$ film**

#### **Determination of the optical band gap for amorphous and nanocrystalline copper oxide thin films prepared by SILAR technique.**

*Rafea, M.A. and Roushdy, N., 2008. Determination of the optical band gap for amorphous and nanocrystalline copper oxide thin films prepared by SILAR technique. Journal of Physics D: Applied Physics, 42(1), p.015413. [5]*

In this study, Amorphous and nanocrystalline copper oxide films were synthesized and characterized utilizing the SILAR technology. The structural and optical properties of the films were examined after being annealed at various temperatures. X-ray diffraction analysis revealed that the films contained both  $Cu_2O$  and  $CuO$  phases[6]. The crystal size was measured to be between 14 and 21 nm. Nano- and micro-sphere-shaped grains were observed in SEM images. After being annealed at 373 K, the amorphous film's band gap grew from 2.3 eV to 2.4 eV. Following the Brus model of energy gap confinement effect, the band gap was shown to steadily shrink to 1.85 eV for annealing temperatures between 373-673 K. The band gap was reduced to 1.7 eV by annealing at 673-823 K, but at a slower rate. The films are well-suited for use as window layers in solar cells due to their increased transmittance spectral window[7].

## 2.4 Heterojunction Solar cell

### **Solution-processed all-oxide nanostructures for heterojunction solar cells**

*Shiu, H.Y., Tsai, C.M., Chen, S.Y. and Yew, T.R., 2011. Solution-processed all-oxide nanostructures for heterojunction solar cells. Journal of Materials Chemistry, 21(44), pp.17646-17650. [8]*

In this study, a new oxide-based material ( $\text{Sn}_{1-x}\text{Co}_x\text{O}_2$ ) was produced for application in heterojunction solar cells via a solution-processing technique. Both p-type copper oxide (p-Cu<sub>2</sub>O) nanostructures and n-type cobalt-doped tin oxide (n-Sn<sub>1-x</sub>Co<sub>x</sub>O<sub>2</sub>) nanoparticles were manufactured using a low-temperature solution technique. Researchers employed hot-press and non-vacuum spray techniques to create inexpensive and scalable n-Sn<sub>1-x</sub>Co<sub>x</sub>O<sub>2</sub>/p-Cu<sub>2</sub>O heterojunction solar cells. Under AM 1.5 lighting, the highest power conversion efficiency (PCE) was 1.2%. As a response to the risks posed by global warming and climate change, the researchers sought to create ecologically acceptable, low-cost solar cell technology[9]. They also worked on creating absorber materials for solar cells that are naturally abundant on Earth. Manufacturing solar cells at large scale and outside of a vacuum is essential for long-term reliability. Using spray and solution techniques for novel absorber layers in oxide-based solar cells, this work gives a solution for low-cost and large-scale applications[10].

## 2.5 Properties of Cu<sub>2</sub>O as thin films

### **Recent advances in cuprous oxide thin film-based photovoltaics.**

*Lakshmanan, A., Alex, Z.C. and Meher, S.R., 2022. Recent advances in cuprous oxide thin film-based photovoltaics. Materials Today Sustainability, 20, p.100244. [11]*

The research paper examines the possibility of thin film photovoltaics as a promising alternative to silicon-based solar cells for the purpose of broad use of solar energy. Cu<sub>2</sub>O (cuprous oxide) emerges as a viable alternative for the quaternary and environmentally detrimental absorber layers in photovoltaic devices[12]. At present, the efficiency of Cu<sub>2</sub>O -based solar cells in laboratory settings has achieved a level of roughly 8%.

However, continuous progress in thin film deposition methods holds promise for enhancing their performance as compared to other solar cell technologies[13].

This report presents a comprehensive survey of advancements in photovoltaic technologies based on  $\text{Cu}_2\text{O}$  over the course of the last ten years. It explores the methodologies adopted by the scientific community to improve the conversion efficiency of conventional solar cells based on  $\text{Cu}_2\text{O}$  / $\text{ZnO}$  heterojunctions [14]. The paper also encompasses various buffer layers that have been extensively documented as effective in mitigating the band offset between the  $\text{Cu}_2\text{O}$  absorber layer and other constituent elements. Moreover, discussion about the present state of endeavors aimed at attaining n-type conductivity in intrinsic p-  $\text{Cu}_2\text{O}$ , with the objective of fabricating solar cells based on homojunctions is also investigated. The paper concludes by suggesting potential avenues for improving device performance, with a specific focus on refining growth processes. In general, this study provides significant perspectives on the progress and prospects of thin film photovoltaics based on  $\text{Cu}_2\text{O}$ [15].

## **2.6 Electrical properties of $\text{Cu}_2\text{O}$**

### **Relationship between the electrical properties of the n-oxide and p- $\text{Cu}_2\text{O}$ layers and the photovoltaic properties of $\text{Cu}_2\text{O}$ -based heterojunction solar cells**

*Minami, T., Miyata, T. and Nishi, Y., 2016. Relationship between the electrical properties of the n-oxide and p- $\text{Cu}_2\text{O}$  layers and the photovoltaic properties of  $\text{Cu}_2\text{O}$ -based heterojunction solar cells. Solar energy materials and solar cells, 147, pp.85-93 [16].*

This research article explores the connection between the photovoltaic performance of  $\text{Cu}_2\text{O}$  -based heterojunction solar cells and the electrical characteristics of the n-oxide semiconductor layer and the p-  $\text{Cu}_2\text{O}$  sheet[17]. A rise in electron concentration in n- $\text{ZnO}$  thin films was found to improve their photovoltaic capabilities up to a point, but subsequently to have a negative effect after that. It was also discovered that changing the annealing temperature and time allowed for regulation of the hole concentration in  $\text{Cu}_2\text{O}$  sheets. The research also revealed that when the hole concentration in  $\text{Cu}_2\text{O}:\text{Na}$  sheets used to make heterojunction solar cells was too high, the cells' photovoltaic characteristics drastically

degraded [18]. The narrowing of the depletion layer and shorter diffusion length were held responsible for the decline. The findings imply that  $\text{Cu}_2\text{O}$ -based heterojunction solar cells can benefit from adjusting the electrical characteristics of the oxide semiconductor and p- $\text{Cu}_2\text{O}$  layers[19]



### 3. DEVICE ARCHITECTURE

Sustainable energy solutions are based mostly on solar energy, and improvements in solar cell technology are essential to raising solar power's price and efficiency. This section concentrates on the architecture of our thin-film solar cell, with a particular emphasis on a setup that includes an active region made of cuprous oxide ( $\text{Cu}_2\text{O}$ ). We hope to obtain a thorough grasp of the mechanism by which sunlight is transformed into electricity in this kind of cell by examining the different layers and their interactions.

The solar cell is made up of multiple designed layers, each with a specific function:

#### 1. Glass Substrate:

The Glass Substrate aids in providing structural support for the cell. It is transparent for maximum light penetration and treated for increased durability and resistance to environmental influences.

#### 2. Fluorine Doped Tin Oxide (FTO):

FTO functions as the bottom electrode and a transparent conductive oxide (TCO). It combines good electrical conductivity and great transparency, allowing light to enter the active zone while reflecting infrared radiation back into the cell, increasing light absorption efficiency.

#### 3. Etched Region:

The purpose of having an etched region is that it assists in the formation of an electrical contact with the top electrode. Sections of the FTO layer are selectively removed to ensure separated electrical contacts, eliminating short circuits and permitting appropriate electrical passage between electrodes. The etched region was on an area of 3mm from the total length of FTO which was 15mm.

#### 4. Titanium Dioxide:

TiO<sub>2</sub> is our p-type layer serving as the ETL. ETL stands for electron transport layer. The electron transport layer is responsible for collecting electrons that are produced in the active region and transporting them to the bottom electrode.

### 5. Cuprous Oxide (Active Layer):

Cuprous Oxide serves as the primary zone for light absorption and electricity generation. Cu<sub>2</sub>O, a semiconductor material with an ideal bandgap, absorbs sunlight, causing electrons to be excited and electron-hole pairs to be formed, which are required for electricity generation.

### 6. Back Metal Contact:

Silver was chosen as the metal contact serving as the final addition to our Solar Cell. This Silver Electrode collects and routes power generated in the active zone to an external circuit. Silver's high electrical conductivity makes it suitable for quickly collecting and transmitting electrical charges, which are commonly arranged in a grid pattern to reduce shading of the active layer.

## 3.1 Device Structure

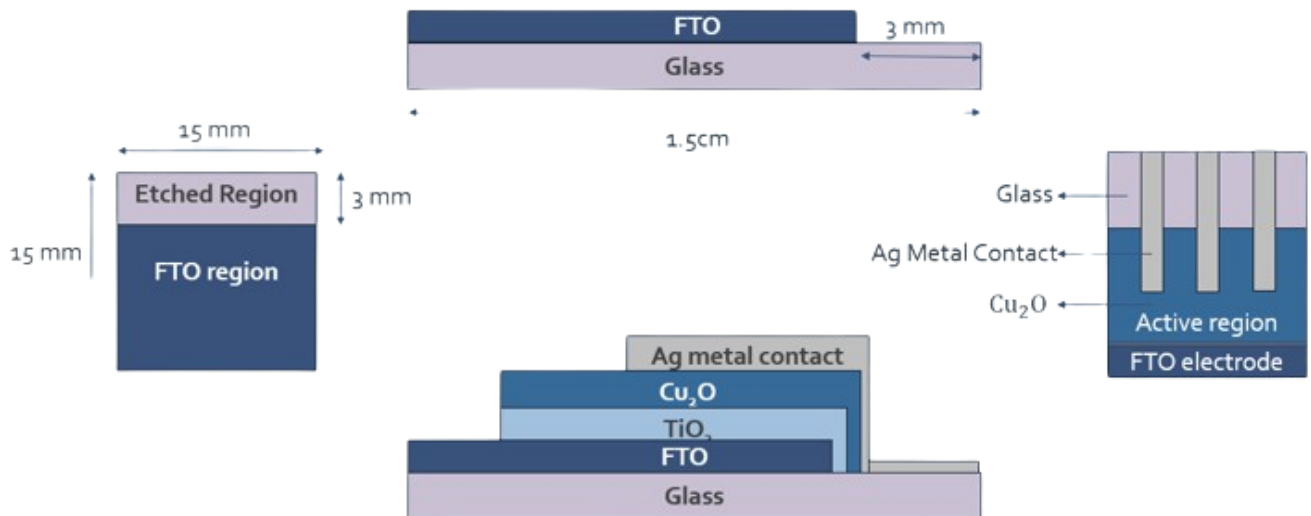


Figure 2 The device model of the heterojunction system.

### 4. METHODOLOGY

As the preceding section entails a detailed explanation of the device model, we now move on towards the Methodology involved in making our Solar Cell Device. This includes Surface Treatment, Synthesis and Deposition of  $\text{Cu}_2\text{O}$  and  $\text{TiO}_2$  on Soda Lime Glass and FTO Glass, Calcination of  $\text{Cu}_2\text{O}$  and  $\text{TiO}_2$  for phase transformation, Thermal Evaporation for the deposition of back metal contact and using Solar Simulation to get I-V Curves.

Solar Cell operates by creating a p-n Junction. For this purpose, we selected Titania as our p-type layer while Cuprous Oxide as our n-type layer. A p-n junction is required for the operation of solar cells because it promotes the separation and movement of charge carriers (electrons and holes) produced by light absorption. In our solar cell design, using titania ( $\text{TiO}_2$ ) as the p-type layer and cuprous oxide ( $\text{Cu}_2\text{O}$ ) as the n-type layer forms a heterojunction, which is fundamental to the cell's operation. These photoactive layers were deposited using the SILAR technique and Spin Coating respectively. In addition, Thermal Evaporation was used to deposit the back metal contacts. The purpose of Back Metal Contacts is to maximize the amount of sunlight captured by the Solar Cell, thereby increasing its efficiency.

#### 4.1 Surface Treatment

The first step in the creation of our Solar Cell Devices is Surface Treatment. This was carried out in several steps. Firstly, we cleaned our samples thoroughly with Ethanol and Acetone. Afterwards, these were put in an Ultrasonic Bath which is a device that uses high frequency ultrasonic waves to clean objects. Sonication was carried out for 30 minutes. Solar Devices must be free from all contaminants thus after Sonication, we carried out Ozone Treatment. Ozone Treatment frees the sample from all contaminants as well as bacteria. Concluding our Surface Treatment process is

Plasma Treatment. Plasma Treatment serves as the final step for surface sterilization as well as Surface Preparation for the deposition of our Photoactive Layers,  $\text{TiO}_2$  and  $\text{Cu}_2\text{O}$ .

## **4.2 Fabrication Of Photoactive Layers**

### **4.2.1 Fabrication and deposition of $\text{Cu}_2\text{O}$ film on Soda lime glass and FTO Glass using SILAR method.**

Many techniques are used to prepare high quality copper oxide thin films such as activated reactive evaporation, thermal oxidation, spray pyrolysis, chemical deposition, sol-gel, electro-deposition, electron beam deposition and pulsed laser deposition and sputtering.

We are using the SILAR method as it is a widely used technique for depositing thin films or layers on substrates, such as a  $\text{Cu}_2\text{O}$  layer on soda lime glass, using a step-by-step methodology.

#### **Materials we need:**

- Soda lime glass 26x35x1 mm<sup>3</sup>
- 0.1 mol. Copper (II) chloride solution: Aqueous solution for copper ion source.
- Sodium hydroxide pH 11.8 solution: Aqueous solution for the reactant.
- Double distilled water
- $\text{H}_2\text{O}_2$  1% solution for oxidation of  $\text{Cu}^{+2}$  ions
- Temperature-controlled hotplate/stirrer: To control the reaction temperature.
- Magnetic stirrer bar: For stirring the solutions.
- Chemical hood: For conducting the process in a controlled environment.
- Glovebox/Nitrogen-filled chamber (if arranged in SCME): To avoid exposure to air and moisture.

#### **Procedure:**

1. Cleaning the Substrate: Clean soda lime glass substrate with alcohol, rinse with Detergent, HCl and deionized water, and dry with nitrogen gas to prevent contamination from water or solvents.
2. Creating a copper (II) chloride solution in deionized water by SILAR process parameters, and a Hydrogen Peroxide solution with 1% solution for deposition.
3. The Three Beaker System:
  - a. The study used high purity copper chloride (AR), ammonium hydroxide, and hydrogen peroxide as metallic copper sources and complex and oxidizing agents.
  - b. The copper chloride will be dissolved in double distilled water and complexed with ammonium hydroxide at a pH of approximately 11.8.
  - c. A 1% H<sub>2</sub>O<sub>2</sub> solution will be used for oxidation.
  - d. The substrate rinsing is done in a beaker with 100 ml double distilled water, changed every 10 cycles to maintain high solution purity. The deposition process will be carried out at room temperature using a three-beakers technique.
  - e. The substrate is dipped vertically in the metallic source for 30 seconds, followed by loosely adsorbed ions.
  - f. The substrate will then be dipped in the double distilled water beaker for 20 seconds, followed by oxidation in the H<sub>2</sub>O<sub>2</sub> beaker for 10 seconds.
  - g. The process was repeated 100 times to achieve the desired thickness. The preparation conditions were optimized by varying dipping times and concentrations.

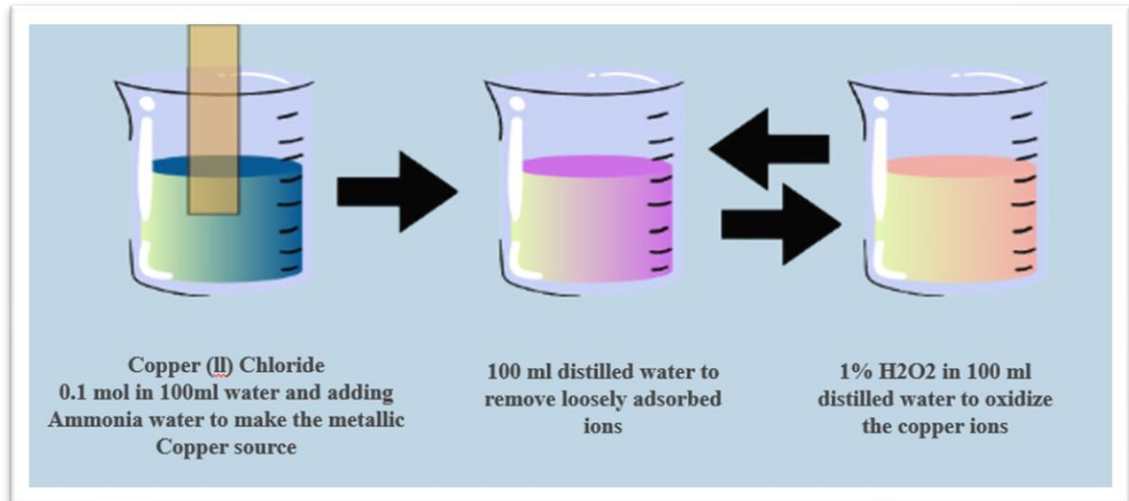


Figure 3 SILAR Method for deposition of Copper (I) Oxide layer

#### 4.2.2 Fabrication and Deposition of TiO<sub>2</sub> using Spin Coating for TiO<sub>2</sub> (TTIP) based acidic solution.

Spin Coating is a popular thin-film deposition method used to cover substrates with thin, even layers of materials. Spin coating utilizes centrifugal forces to deposit the required material on the substrate. When using Titanium Oxide (TiO<sub>2</sub>) on Titanium Isopropoxide (TTIP) in an acidic solution, followings steps will be followed as directed to us by [20]:

##### 1. Preparation of substrate

The substrate is made completely free of any impurities by thorough cleaning. For cleaning, we can use solvents such as acetone, isopropanol, and deionized water. Nitrogen gas or compressed air can be used for drying it afterwards.

##### 2. Mounting the substrate:

The cleaned substrate is placed on the chuck of the spin-coating machine. The substrate is set in position through the vacuum generated by the chuck. Afterwards, the rotation speed is set based on the specific requirements for film thickness and uniformity.

### **3. Dropping the solution:**

The solution/suspension material is placed above the rotating substrate. Height between the container and the substrate's surface plays a crucial role in achieving the desired film thickness, therefore It must be carefully kept. The solution is dropped onto the rotating substrate afterwards.

### **4. Spin-Up and Spin-Off:**

Spin-Up phase is initiated. In it, the spin coater rapidly accelerates the rotation of the substrate. This results in the creation of a centripetal force that causes the solution to spread out and coat the substrate uniformly. The desired spin-speed is maintained for a specific duration for uniform coating. This is called Spin-off.

### **5. Evaporation:**

This may be an optional step to remove residual solvents or to enhance film properties.

### **6. Characterization and testing:**

Characterization techniques such as XRD, SEM, UV-Vis Spectroscopy are used to check the quality, thickness and other required specifications of the thin film.

### **7. Post Processing:**

Optimization and layering of spin-coating process may be done, depending upon the application. Additional steps such as surface functionalization or others are carried out if post-processing is required.

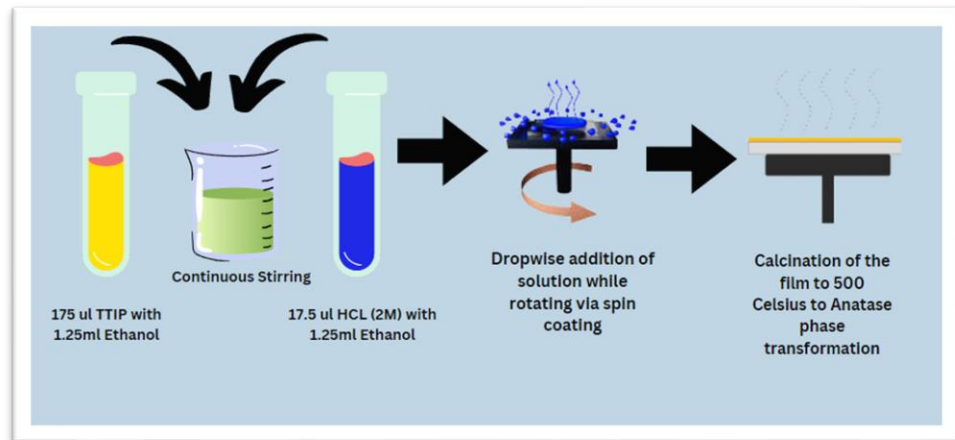


Figure 4 Method of Deposition of Titania

#### 4.2.3 Calcination of $\text{TiO}_2$ and $\text{Cu}_2\text{O}$ for Phase Transformation

After the deposition of each Photoactive layer, the next step was to calcinate them in order to ensure proper adhesion and to achieve the desired characteristics. Both the Photoactive layers were calcinated in a Muffle Furnace.  $\text{TiO}_2$  was calcinated first at a temperature of 500 Degrees Celsius while  $\text{Cu}_2\text{O}$  was calcinated at a temperature of 200 Degrees Celsius. The differences between the surface morphologies of our Photoactive Layers with and without calcination are explained thoroughly in the forthcoming chapter of characterization and results.

#### 4.2.4 Thermal Evaporation for back metal contacts

Thin films are often deposited by thermal evaporation. It can create back metal connections for solar cells and other electronics. We have made a step-by-step thermal evaporation for rear metal contacts:

##### 1. Substrate Cleaning:

For optimal adhesion and electrical contact, the substrate (usually a semiconductor material) must be cleaned before metal deposition. Ultrasonic cleaning with acetone, isopropanol, or deionized water and nitrogen blow drying are common procedures.

##### 2. Readyng the Vacuum Chamber and Metal Source Preparation:



We must make sure the vacuum chamber is clean. A "dummy" run to clear the chamber by evaporating a little metal before deposition may be helpful. Lowering the vacuum chamber pressure to  $10^{-6}$  Torr or superior. Putting aluminum, silver, gold, etc. in a tungsten boat or crucible to evaporate. Keep metal pure to avoid impurities.

### **3. Thermal Evaporation:**

Gradually heat the metal with electricity to evaporation temperature. Evaporating metal atoms condense on the cooler substrate above. Check metal layer thickness with a quartz crystal monitor to guarantee appropriate thickness.

### **4. Ventilation and cooling:**

Stop evaporation and cool the chamber and substrate after reaching the desired thickness. To avoid moisture and impurities, slowly exhaust the chamber with dry nitrogen.

### **5. Characterization:**

SEM, AFM, and XRD can assess film shape, thickness, and crystallinity.

Post-deposition annealing may improve the contact's electrical properties or substrate adherence. Annealing can be done in vacuum, nitrogen, or forming gas depending on desired qualities. We must note that the stages and conditions may vary according to the device being made, the metal being evaporated, and the intended product qualities.

#### **4.2.5 Solar Simulation for I-V Curves**

Thermal Evaporation concludes the making of our Solar Cell device. Afterwards, our purpose was to generate I-V Curves showcasing the efficiency of our devices. For this purpose, Solar Simulation was carried out. The detailed explanation about the I-V Curve graphs along with the results will be discussed in the forthcoming section of Solar Simulation.

5. TESTING AND RESULTS

5.1 Characterization of Titania layer (N-Type)

5.1.1 Scanning Electron Microscopy (SEM)

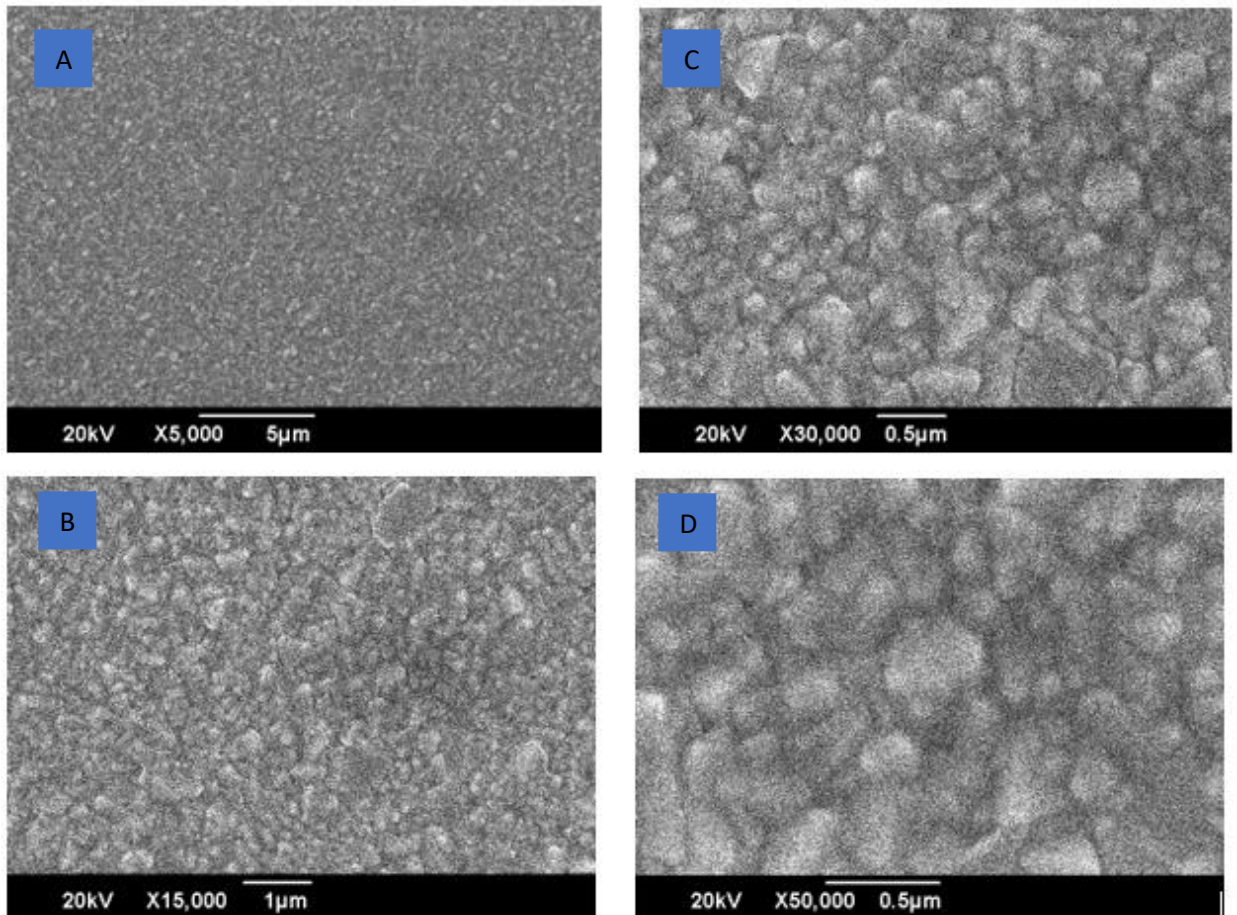


Figure 5 SEM images for magnification A) x5000 B) x15000 C) x30000 D) x50000

- **Explanation:**

The SEM images provide valuable insights into the Titania ( $\text{TiO}_2$ ) coating on the FTO (Fluorine-doped Tin Oxide) glass substrate:

### **1. Surface Morphology:**

- The images reveal that the TiO<sub>2</sub> coating consists of a dense layer of nanoparticles.
- The nanoparticles are relatively uniform in size and shape, suggesting good control over the spin coating process.
- The surface appears to be rough, which is beneficial for light trapping in solar cell applications.

### **2. Particle Size:**

- The particle size appears to be in the nanometer range, as evidenced by the increasing resolution of the images.
- The higher magnification images (X30,000 and X50,000) show individual particles with sizes estimated to be around 20-50 nanometers. This is ideal for forming a mesoporous structure.

### **3. Coating Thickness:**

- While the exact thickness cannot be determined from the SEM images alone, the cross-sectional view (if available) would provide this information.
- The high magnification images suggest that the coating is relatively thin, possibly on the order of hundreds of nanometers.

## **5.1.2 Energy dispersive X-ray spectroscopy**

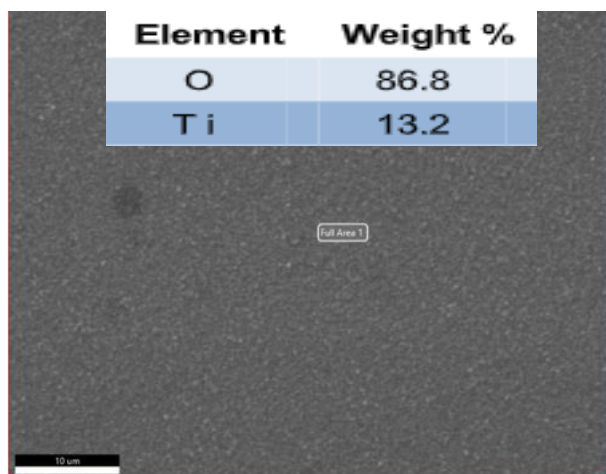


Figure 6 Elemental composition for Titania

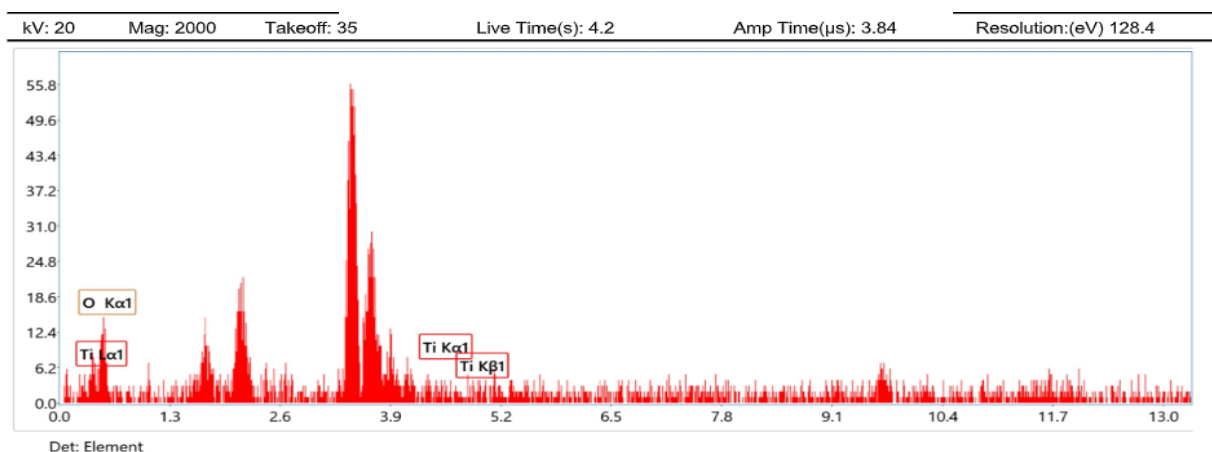


Figure 7 EDX results for Titania

### Explanation:

The EDX results, coupled with the SEM image, provide insights into the chemical composition and distribution of the elements within the  $\text{TiO}_2$  coating on FTO glass substrate.

1. **Elemental Composition:** The EDX analysis reveals the presence of two main elements: Titanium (Ti) and Oxygen (O). This confirms the formation of Titanium dioxide ( $\text{TiO}_2$ ) which is the desired material for the photoactive layer.

2. **Quantitative Analysis:** The quantitative results show that the coating is primarily composed of oxygen (86.8 wt. %) and titanium (13.2 wt. %), closely matching the expected stoichiometry of  $\text{TiO}_2$  ( $\text{TiO}_2$  is ideally composed of 1 Ti atom and 2 O atoms, with about 60wt% O, and 40wt% Ti).
3. **Purity:** The absence of significant peaks for other elements indicates that the coating is relatively pure, with no major impurities detected within the sensitivity limits of the EDX analysis.
4. **Distribution:** The SEM image suggests a uniform distribution of Ti and O across the analyzed area, indicating a homogeneous coating. The granular appearance in the image could be due to the nanocrystalline nature of the  $\text{TiO}_2$  film.

### 5.1.3 UV-VIS Spectroscopy

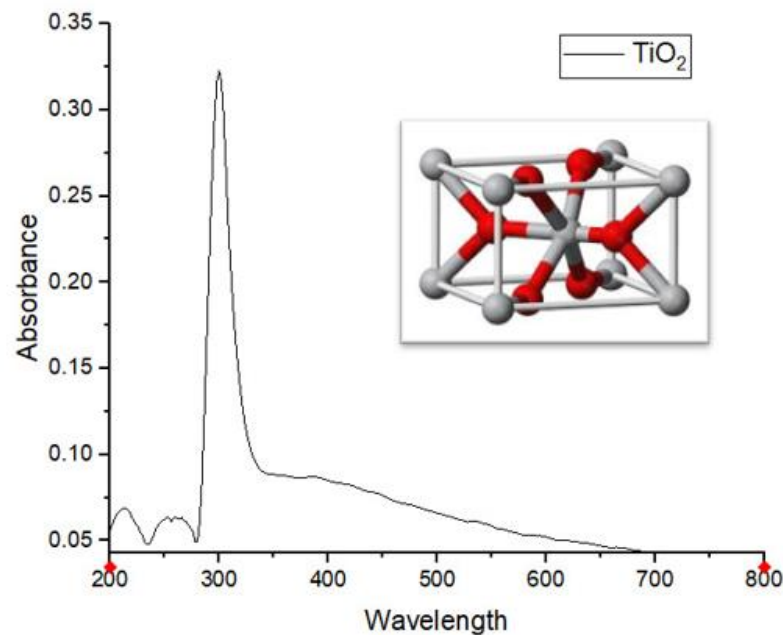


Figure 8 Absorbance vs Wavelength graph for Titania

### Explanation:

The UV-Vis spectroscopy results of the TiO<sub>2</sub> coated FTO glass show the following key features:

1. **Strong Absorption in the UV Region:** The TiO<sub>2</sub> coating exhibits strong absorption below 400 nm, which corresponds to the ultraviolet (UV) region of the electromagnetic spectrum. This is consistent with the electronic band structure of TiO<sub>2</sub>, where the energy difference between the valence band and conduction band (band gap) is typically around 3.0-3.2 eV for anatase TiO<sub>2</sub>. This band gap energy corresponds to a photon wavelength of around 387-413 nm.
2. **Decreasing Absorption Towards Visible Light:** As the wavelength increases beyond 400 nm and into the visible light region, the absorbance of the TiO<sub>2</sub> coating gradually decreases. This indicates that TiO<sub>2</sub> primarily absorbs higher energy photons in the UV range and has limited absorption capacity for lower energy photons in the visible range.
3. **Optical Band Gap Estimation:** The optical band gap of the TiO<sub>2</sub> coating can be estimated by extrapolating the linear portion of the absorption edge in the Tauc plot (plot of  $(\alpha h\nu)^2$  vs.  $h\nu$ , where  $\alpha$  is the absorption coefficient,  $h$  is Planck's constant, and  $\nu$  is the frequency of light). The intercept of this linear extrapolation with the x-axis gives an estimate of the band gap energy.

### 5.1.4 RAMAN Spectroscopy

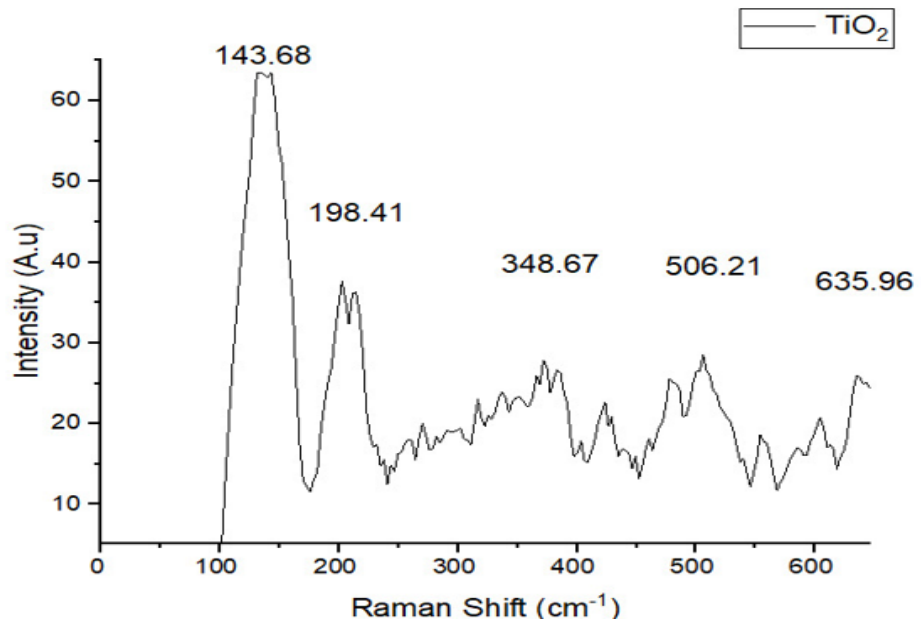


Figure 9 RAMAN spectroscopy for Titania

#### Explanation:

The Raman spectrum you provided offers valuable information about the TiO<sub>2</sub> coating on FTO glass, which is intended to serve as the n-type photoactive layer in an all-oxide solar cell.

- **Anatase Phase:** The peaks observed at 143.68 cm<sup>-1</sup>, 198.41 cm<sup>-1</sup>, 348.67 cm<sup>-1</sup>, 506.21 cm<sup>-1</sup>, and 635.96 cm<sup>-1</sup> are characteristic Raman modes of anatase TiO<sub>2</sub>. This is the most desirable phase for photocatalytic and photovoltaic applications due to its superior charge carrier mobility and higher surface area compared to the rutile phase.
- **High Crystallinity:** The sharp and well-defined peaks suggest a high degree of crystallinity in the TiO<sub>2</sub> coating. Crystallinity is important for efficient charge transport, as it minimizes defects that can act as recombination centers for photogenerated electrons and holes.

- **No Impurity Phases:** The absence of additional peaks indicates the absence of other TiO<sub>2</sub> polymorphs like rutile or brookite, as well as any significant impurities. This suggests the formation of a pure anatase TiO<sub>2</sub> phase.



## 5.2 Characterization of Copper 1 Oxide layer (P-Type)

### 5.2.1 Scanning Electron Microscopy (SEM)

- 100 cycles of Non Calcinated layer

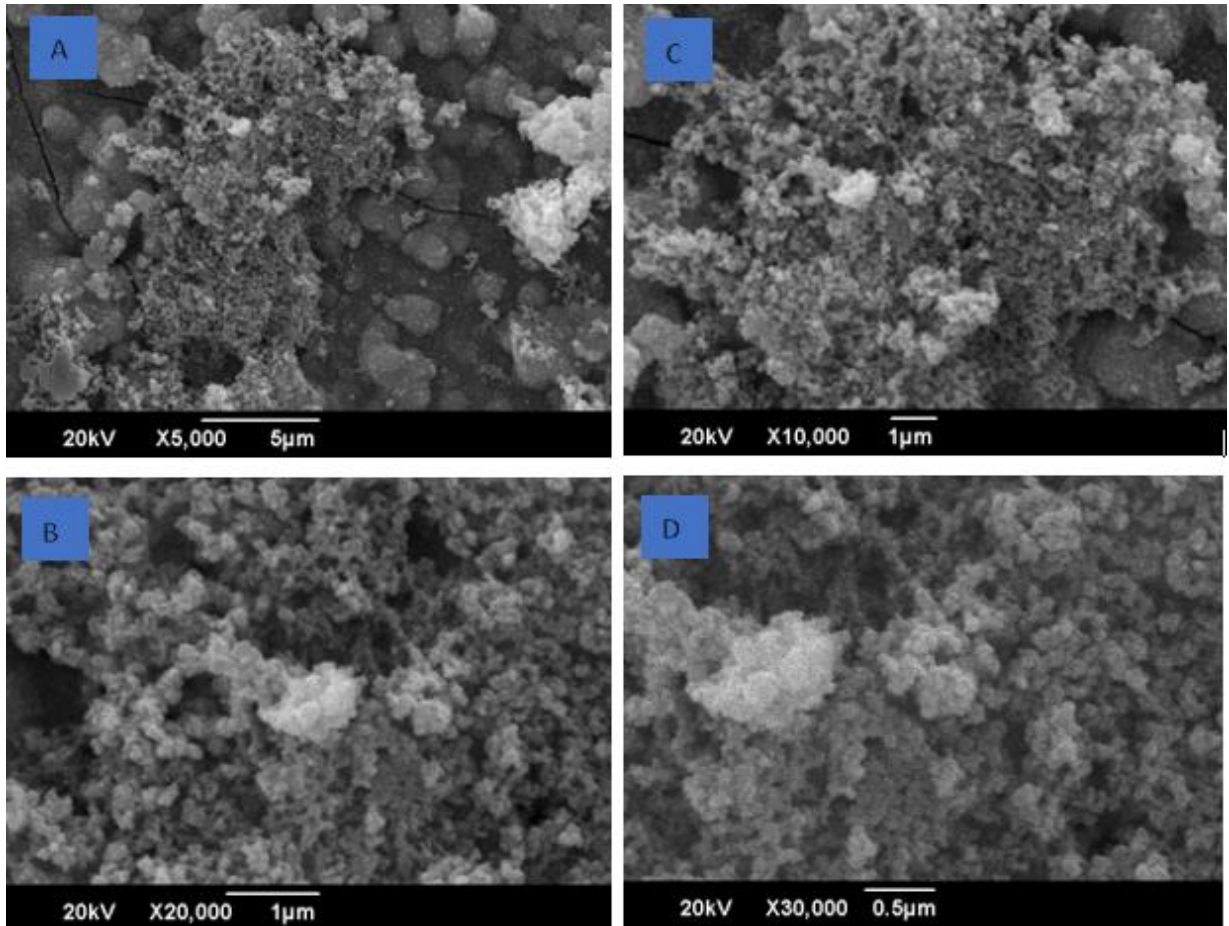


Figure 10 SEM Images on magnification A) x5000 B) x20000 C) x10000 D) x30000

#### **Explanation:**

The SEM images of the non-calcined copper(I) oxide ( $\text{Cu}_2\text{O}$ ) coating on FTO glass, deposited using 100 SILAR cycles, reveal the following:

#### **Morphology:**

- **Non-uniform Coating:** The images show a non-uniform and uneven distribution of the  $\text{Cu}_2\text{O}$  coating on the FTO substrate. This is evident from the varying density and sizes of the particles across the surface.

- **Agglomeration:** The particles tend to agglomerate, forming clusters rather than a smooth and continuous layer. This agglomeration can lead to voids and pinholes in the film, potentially affecting its electrical and optical properties.
- **Rough Surface:** The surface of the coating appears rough and porous, which can increase surface area but might also lead to scattering and trapping of light, hindering efficient charge collection.
- **Particle Size and Shape:** The particles exhibit a range of sizes and shapes, indicating poor control over the growth process. This can result in a wide distribution of energy levels and affect the overall electronic properties of the film.
- **100 cycles of Calcinated layer**

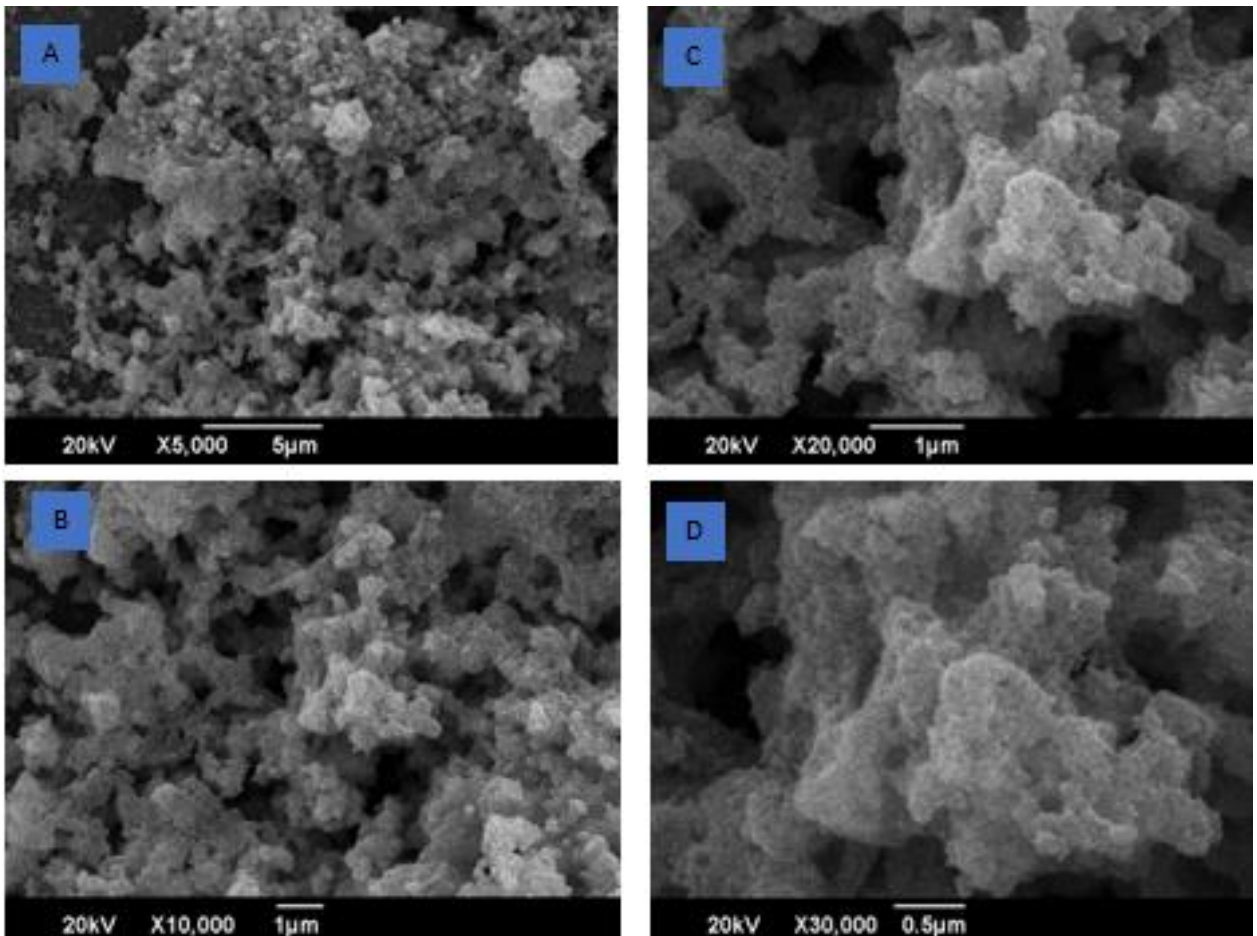


Figure 11 SEM Images on magnification A) x5000 B) x10000 C) x20000 D) x30000

## **Explanation:**

The SEM images of the calcined copper(I) oxide ( $\text{Cu}_2\text{O}$ ) coating deposited using 100 SILAR cycles show distinct improvements compared to the non-calcined sample:

## **Morphology:**

- **Enhanced Uniformity:** The coating appears more uniform and evenly distributed across the FTO substrate, with less variation in particle density and size compared to the non-calcined sample. This indicates better adhesion and a more continuous film formation.
- **Reduced Agglomeration:** While some agglomeration is still visible, it is significantly reduced compared to the non-calcined sample. The particles are less clustered, and the film appears denser, suggesting fewer voids and pinholes.
- **Smoother Surface:** The surface of the calcined  $\text{Cu}_2\text{O}$  film is smoother and less porous than the non-calcined one. This can lead to improved light absorption and charge collection due to reduced scattering and trapping of light.
- **More Defined Particle Shape:** The particles exhibit a more defined and uniform shape, typically spherical or cubic, suggesting better control over the growth process and a more homogeneous distribution of energy levels.

- **200 cycles of Non Calcinated layer:**

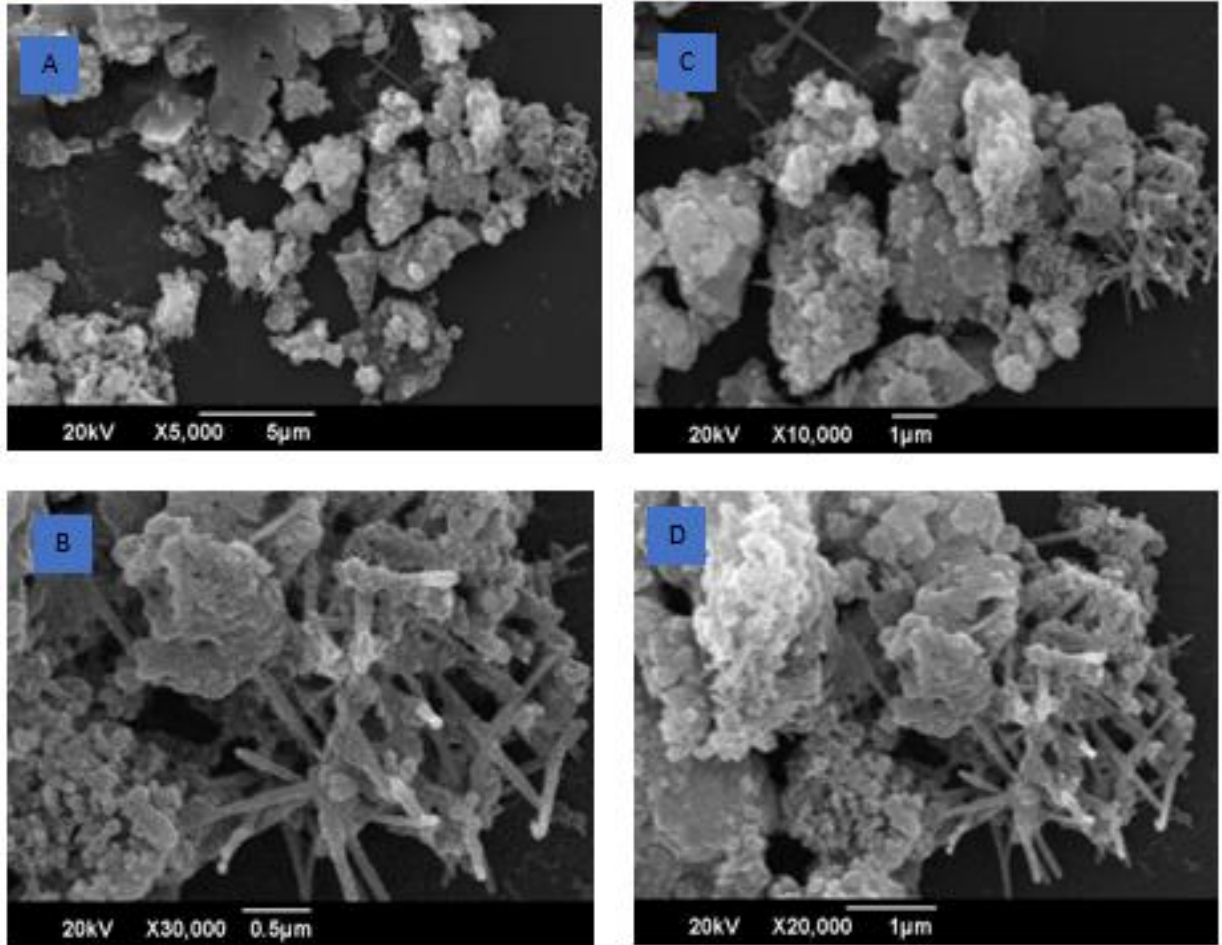


Figure 12 SEM Images for magnification A) x5000 B) x30000 C) x10000 D) x20000

### **Explanation:**

The SEM images of the non-calcined copper(I) oxide ( $\text{Cu}_2\text{O}$ ) coating deposited using 200 SILAR cycles reveal the following:

### **Morphology:**

- **Non-uniform Coating:** The images show a non-uniform and uneven distribution of the  $\text{Cu}_2\text{O}$  coating on the FTO substrate, particularly at lower

magnifications (5,000x and 10,000x). The coating appears denser in some areas and sparse in others.

- **Agglomeration:** The Cu<sub>2</sub>O particles exhibit significant agglomeration, forming large clusters and aggregates. This is evident in all magnifications but is particularly pronounced at higher magnifications (20,000x and 30,000x).
- **Rough Surface:** The surface of the coating appears rough and uneven due to the agglomeration and irregular particle shapes.
- **Diverse Particle Shapes:** The particles exhibit a wide range of shapes, including spherical, rod-like, and irregular structures. This suggests uncontrolled growth and a lack of uniformity in the particle formation process.

#### **Comparison with 100 Cycles (Non-Calcined):**

- **Increased Agglomeration:** The 200-cycle non-calcined sample shows a higher degree of agglomeration compared to the 100-cycle sample. The particles are larger and form denser clusters.
- **More Diverse Particle Shapes:** The 200-cycle sample exhibits a wider variety of particle shapes compared to the 100-cycle sample, indicating less control over the growth process.

- **200 cycles of Calcinated layer:**

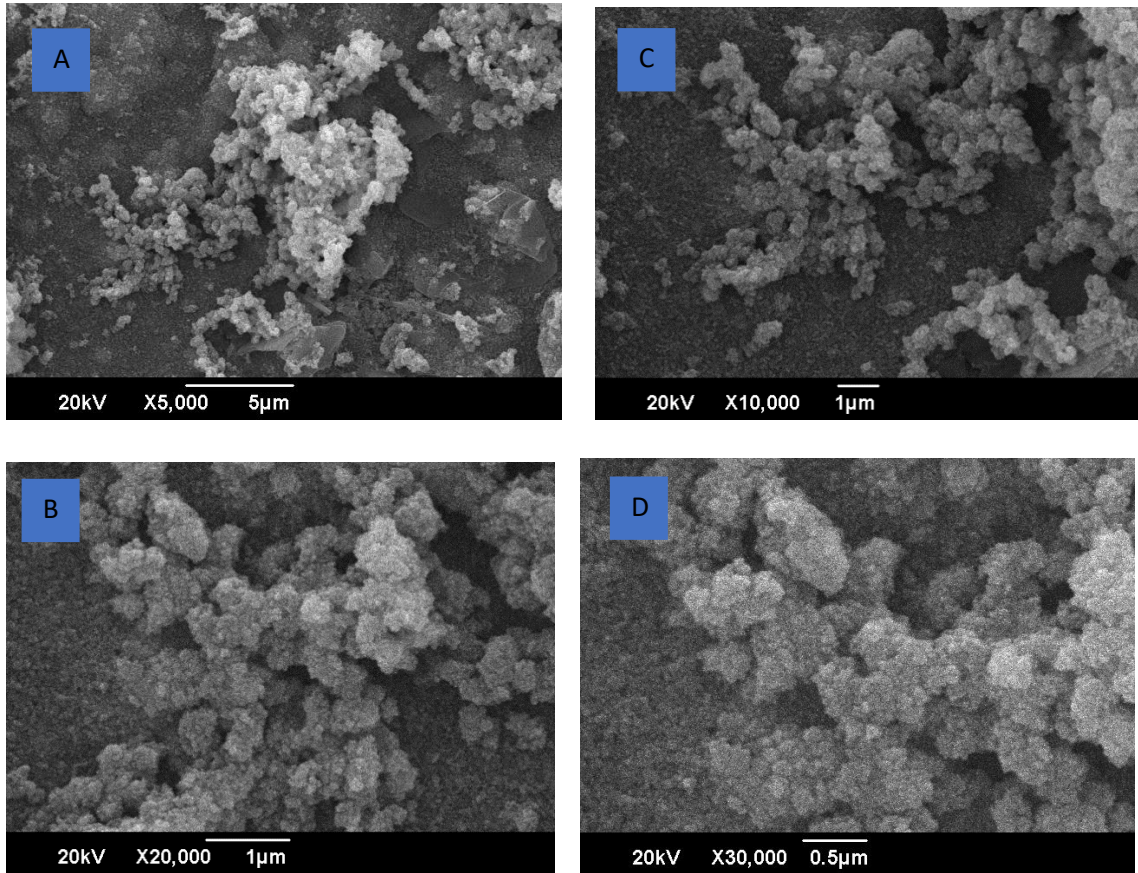


Figure 13 SEM Images for magnification A) x5000 B) x20000 C) x10000 D) x30000

### **Explanation:**

The SEM images of the calcined copper(I) oxide ( $\text{Cu}_2\text{O}$ ) coating deposited using 200 SILAR cycles reveal a significant improvement in morphology compared to the non-calcined samples:

### **Morphology:**

- **Enhanced Uniformity and Coverage:** The coating appears highly uniform and covers the FTO substrate comprehensively, with consistent particle

density and size distribution across the entire surface. This suggests excellent adhesion and continuous film formation.

- **Minimal Agglomeration:** The degree of agglomeration is significantly reduced compared to both non-calcined samples. The particles are well-dispersed, and the film exhibits a compact and dense structure with minimal voids or pinholes.
- **Smooth Surface:** The surface of the calcined  $\text{Cu}_2\text{O}$  film is remarkably smooth and uniform, indicating a well-ordered arrangement of particles. This smoothness can enhance light absorption and minimize scattering.
- **Well-Defined Cubic Particles:** The particles predominantly exhibit a cubic morphology with well-defined edges and corners, suggesting a high degree of crystallinity and controlled growth during calcination.

### 5.2.2 Energy dispersive X-ray spectroscopy

- **100 cycles of Non Calcinated layer:**

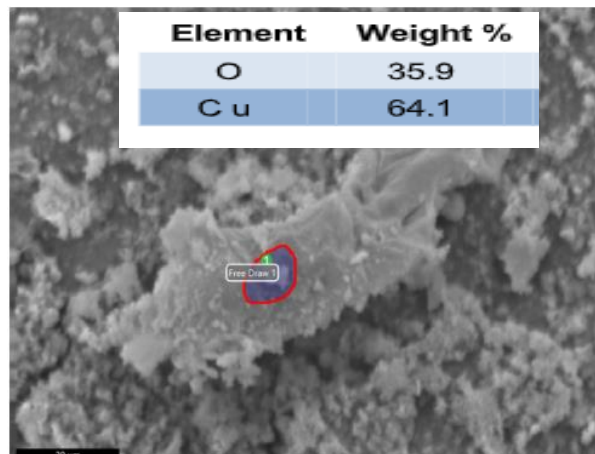


Figure 14 Elemental composition of Copper (I) Oxide at 100 Non-Calcinated

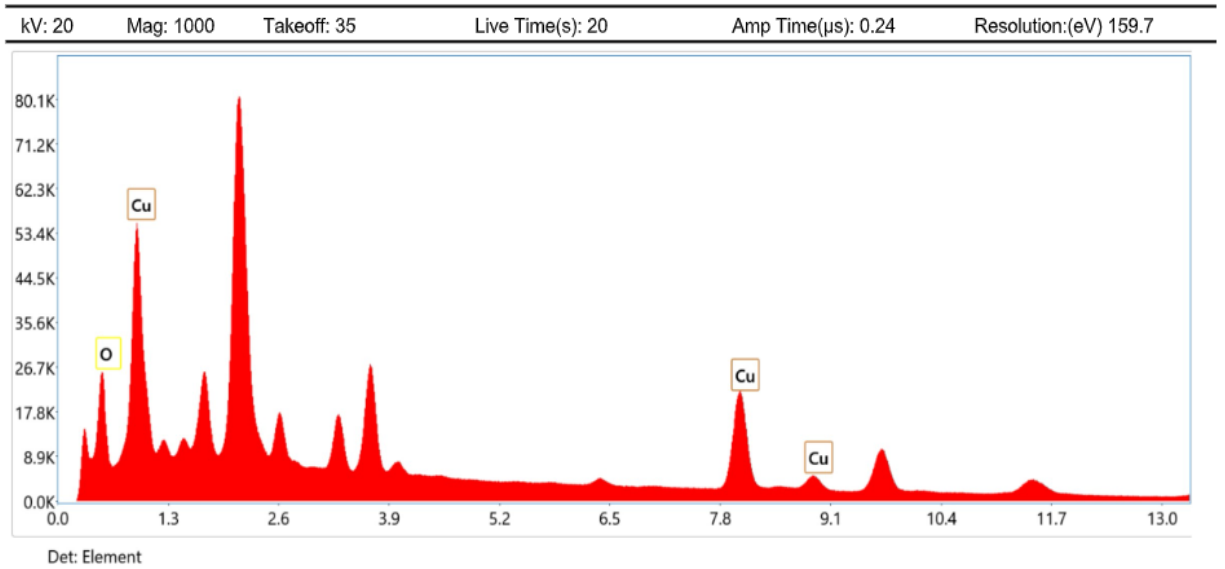


Figure 15 EDX Results for Copper (I) Oxide at 100 Non-Calcinated

### Explanation:

The EDX results for the non-calcined copper(I) oxide ( $\text{Cu}_2\text{O}$ ) coating deposited using 100 SILAR cycles reveal the following insights:

### Composition:

- **Copper and Oxygen Presence:** The presence of copper (Cu) and oxygen (O) peaks confirms the formation of copper oxide on the FTO substrate.
- **$\text{Cu}_2\text{O}$  Stoichiometry Deviation:** The weight percentages of Cu (64.1%) and O (35.9%) deviate from the ideal stoichiometry of  $\text{Cu}_2\text{O}$  (Cu: 88.8%, O: 11.2%). This suggests an excess of copper or a copper-rich phase in the coating.

### Implications:

- **Non-Ideal Composition:** The deviation from the ideal  $\text{Cu}_2\text{O}$  stoichiometry can lead to the formation of other copper oxide phases (like CuO) or the presence



of unreacted copper, both of which can be detrimental to the photovoltaic performance of the material.

- **Potential for Defects:** Excess copper can lead to the formation of defects like copper vacancies or interstitials, which can act as recombination centers and hinder charge transport.
- **Impact on Band Gap:** The non-stoichiometry can also affect the band gap of the material, potentially shifting the absorption edge and reducing the efficiency of light absorption.

**100 Calcinated:**

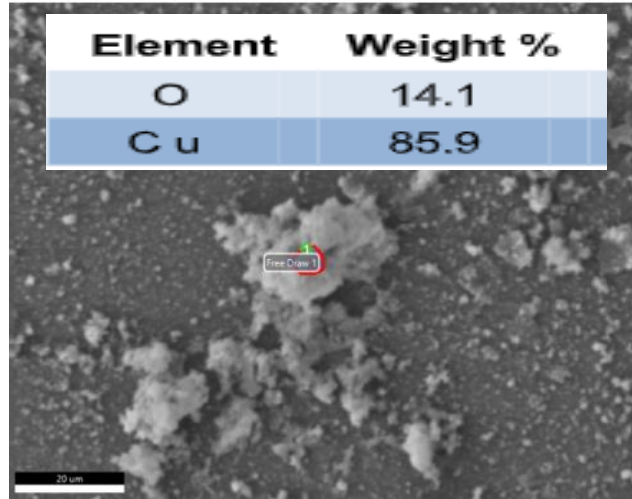


Figure 16 Elemental Composition of Copper (I) oxide at 100 Calcinated

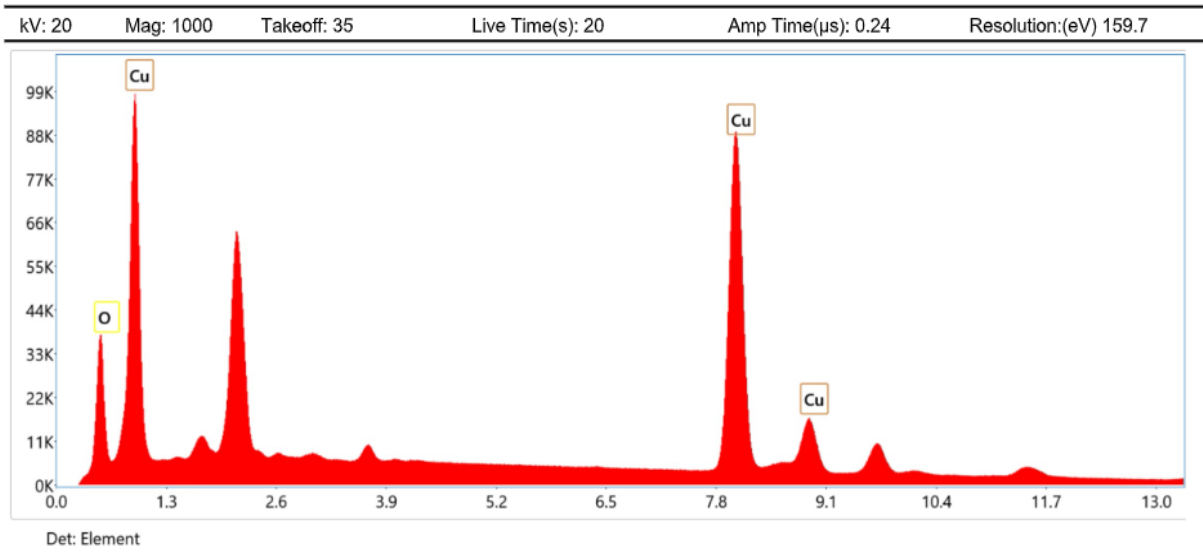


Figure 17EDX Results for Copper(I)Oxide at 100 Calcinated

**Explanation:**

The EDX results for the 100-cycle calcined copper(I) oxide ( $\text{Cu}_2\text{O}$ ) coating reveal the following insights:

### Composition:

- **Primarily Copper and Oxygen:** The main peaks in the spectrum correspond to copper (Cu) and oxygen (O), confirming the presence of copper oxide on the FTO substrate.
- **Improved Stoichiometry:** The weight percentages of Cu (85.9%) and O (14.1%) are closer to the ideal stoichiometry of Cu<sub>2</sub>O (Cu: 88.8%, O: 11.2%) compared to the non-calcined sample. This indicates a higher purity of Cu<sub>2</sub>O in the calcined film.

### Implications:

- **Enhanced Cu<sub>2</sub>O Formation:** The improved stoichiometry suggests that calcination successfully promoted the formation of Cu<sub>2</sub>O and reduced the presence of other copper oxide phases or unreacted copper.
- **Fewer Defects:** The closer-to-ideal composition implies a lower likelihood of defects like copper vacancies or interstitials, which can hinder charge transport and reduce efficiency.
- **More Favorable Band Gap:** The improved stoichiometry is expected to lead to a band gap closer to the optimal value for Cu<sub>2</sub>O, enhancing light absorption and charge generation.

## 200 Non Calcinated:

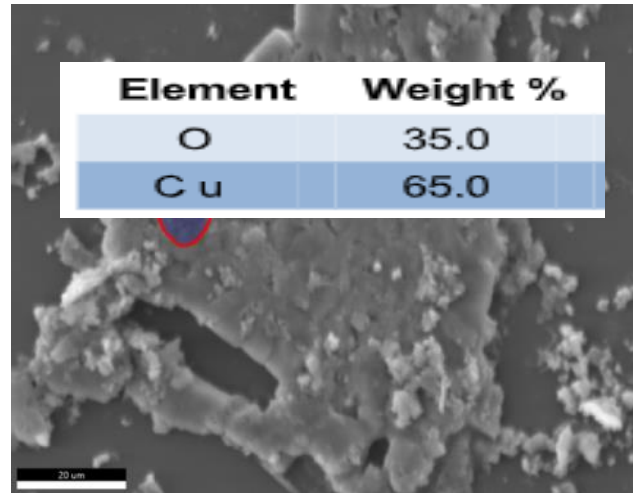


Figure 18 Elemental Composition of Copper (I) Oxide at 200 Non-Calcinated

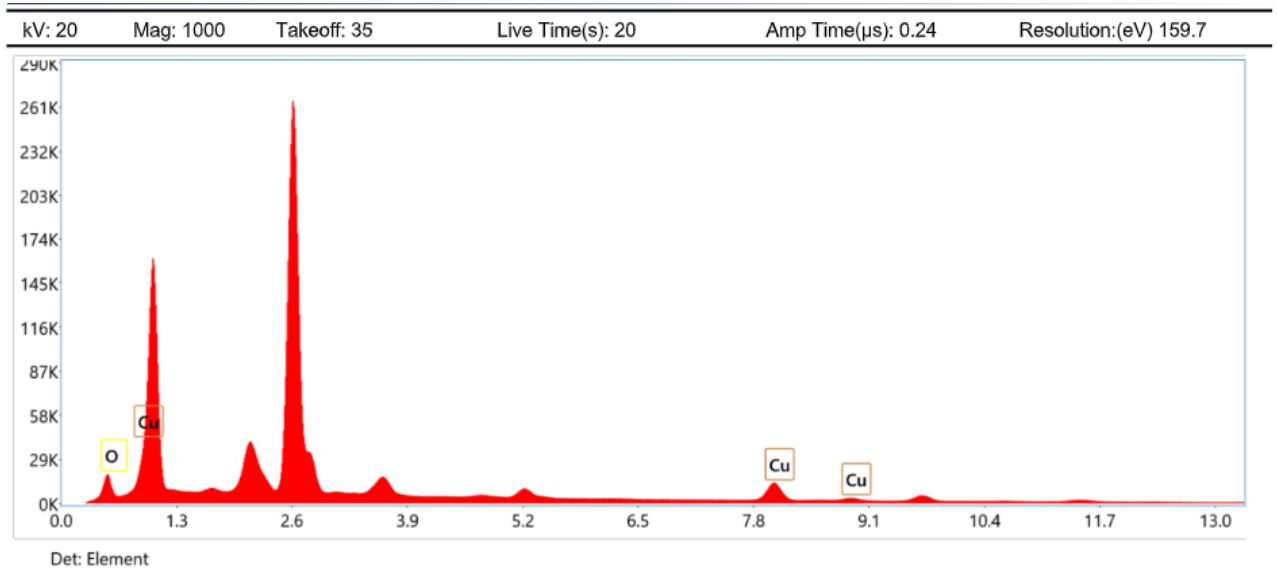


Figure 19 EDX Results for Copper (I) Oxide at 200 Non-Calcinated

## Explanation:

The EDX results for the 200-cycle non-calcined copper(I) oxide ( $\text{Cu}_2\text{O}$ ) coating reveal the following insights:

### Composition:

- **Primarily Copper and Oxygen:** The main peaks in the spectrum correspond to copper (Cu) and oxygen (O), confirming the presence of copper oxide on the FTO substrate.
- **Deviation from Ideal Stoichiometry:** The weight percentages of Cu (65.0%) and O (35.0%) deviate significantly from the ideal stoichiometry of  $\text{Cu}_2\text{O}$  (Cu: 88.8%, O: 11.2%). This indicates a copper-rich composition, suggesting the presence of other copper oxide phases (like  $\text{CuO}$ ) or unreacted copper.

### Implications:

- **Non-Ideal Composition:** The deviation from the ideal  $\text{Cu}_2\text{O}$  stoichiometry suggests a less pure film with potential for the presence of multiple copper oxide phases. This can negatively impact the optoelectronic properties of the material.
- **Increased Defects:** The excess copper can lead to the formation of defects like copper vacancies **or interstitials, which can act as** recombination centers for charge carriers and hinder efficient charge transport.
- **Impact on Band Gap:** The non-stoichiometric composition can alter the band gap of the material, potentially shifting the absorption edge and affecting the efficiency of light absorption.

## 200 Calcinated:

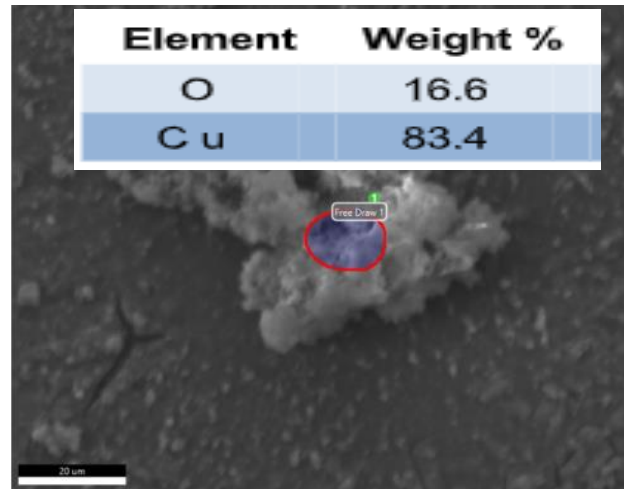


Figure 20 Elemental composition of Copper (I) Oxide at 200 Calcinated

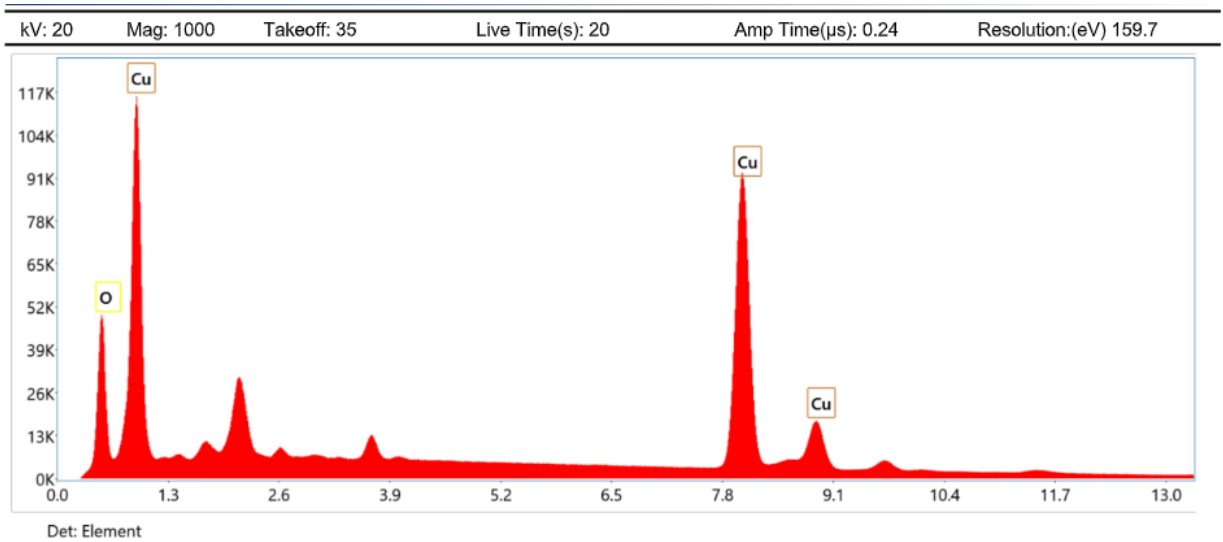


Figure 21 EDX Results for Copper (I) Oxide at 200 Calcinated

### Explanation:

The EDX results for the 200-cycle calcined copper(I) oxide ( $\text{Cu}_2\text{O}$ ) coating reveal the following insights:

### Composition:

- **Primarily Copper and Oxygen:** The main peaks in the spectrum correspond to copper (Cu) and oxygen (O), confirming the presence of copper oxide on the FTO substrate.
- **Near-Ideal Stoichiometry:** The weight percentages of Cu (83.4%) and O (16.6%) are very close to the ideal stoichiometry of  $\text{Cu}_2\text{O}$  (Cu: 88.8%, O: 11.2%). This indicates a high purity of  $\text{Cu}_2\text{O}$  in the calcined film and successful formation of the desired copper oxide phase.

### **Implications:**

- **High-Quality  $\text{Cu}_2\text{O}$  Formation:** The near-ideal stoichiometry suggests that calcination with 200 cycles has successfully promoted the formation of pure  $\text{Cu}_2\text{O}$  with minimal presence of other copper oxide phases or unreacted copper.
- **Minimized Defects:** The close-to-ideal composition implies a lower likelihood of defects like copper vacancies or interstitials, which can hinder charge transport and reduce efficiency.
- **Optimal Band Gap:** The improved stoichiometry is expected to result in a band gap very close to the optimal value for  $\text{Cu}_2\text{O}$ , maximizing light absorption and charge generation.

### 5.2.3 UV-Vis Spectroscopy

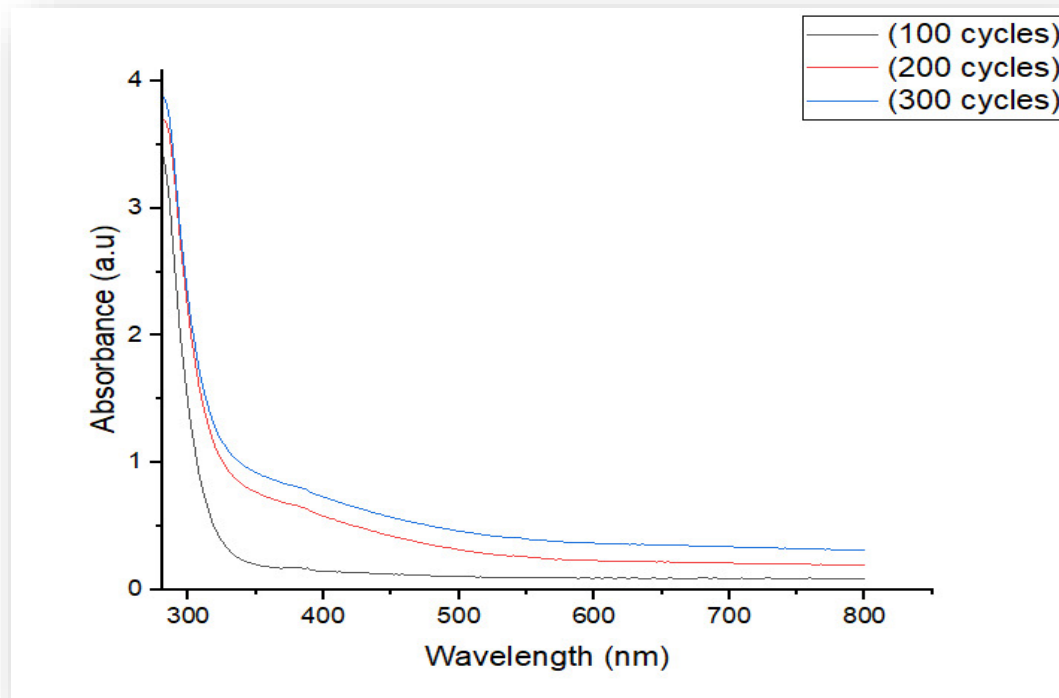


Figure 22 Absorbance vs Wavelength graph for Copper (I) Oxide at different Cycles

#### Explanation:

The UV-Vis spectroscopy results of the  $\text{Cu}_2\text{O}$  coatings provide insights into their optical properties and suitability as p-type photoactive layers for all-oxide solar cells. Let's analyze the two graphs separately:

#### Graph 1: Effect of SILAR Cycles (100, 200, 300)

- **Absorption Trends:** All three samples show strong absorption in the UV region (<400 nm) and a gradual decrease in absorption towards the visible and near-infrared regions. This is characteristic of  $\text{Cu}_2\text{O}$ , a semiconductor with a direct bandgap around 2.1 eV.



- **Increasing Absorbance with Cycles:** The absorbance increases with the number of SILAR cycles, indicating thicker films with more material to absorb light. This is expected as more cycles lead to greater deposition of  $\text{Cu}_2\text{O}$ .

### Graph 2: Calcined vs. Non-Calcined layers

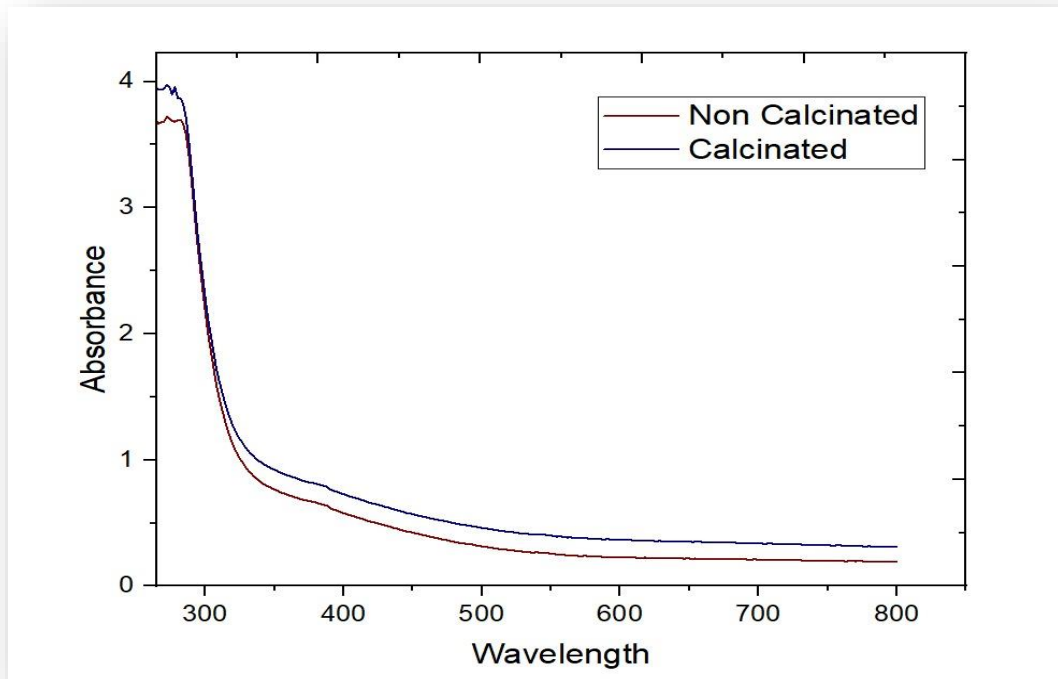


Figure 23 Absorbance vs Wavelength graph for Calcinated and Non-Calcinated Copper (I) Oxide

- **Enhanced Absorption after Calcination:** The calcined sample exhibits significantly higher absorbance across the entire spectrum compared to the non-calcined sample. This suggests that calcination improves the crystallinity and reduces defects in the  $\text{Cu}_2\text{O}$  film, leading to better light absorption properties.
- **Sharper Absorption Edge:** The absorption edge of the calcined sample is sharper, indicating a more defined bandgap and better-defined electronic transitions. This is consistent with the improved crystallinity expected from calcination.

### Implications for All-Oxide Solar Cells:

- **Thickness Control:** The first graph demonstrates that the thickness of the  $\text{Cu}_2\text{O}$  layer can be controlled by varying the number of SILAR cycles. This allows for optimization of the layer thickness to balance light absorption and charge carrier collection.
- **Calcination Improves Performance:** The second graph shows that calcination is crucial for enhancing the light absorption properties of  $\text{Cu}_2\text{O}$ . The increased absorbance and sharper absorption edge of the calcined sample are desirable for efficient solar energy conversion.

### Tauc Plot:

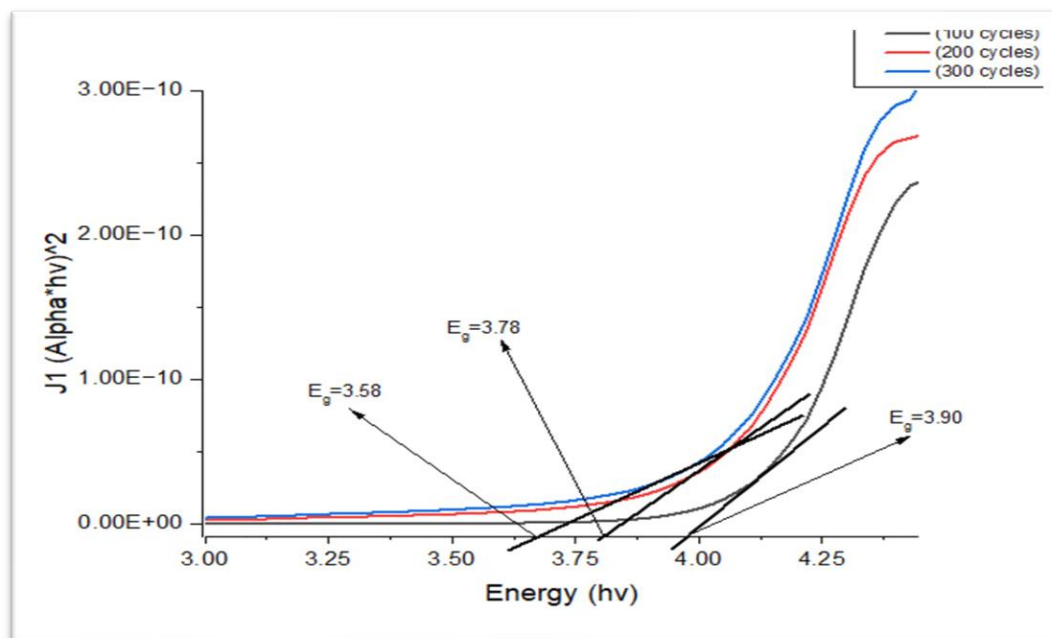


Figure 24 Tauc Plot showing Energy Gap values at different cycles

## **Explanation:**

The Tauc plots illustrate the relationship between photon energy and the modified absorption coefficient for copper(I) oxide ( $\text{Cu}_2\text{O}$ ) films deposited on FTO glass using SILAR. These plots are used to estimate the optical bandgap, a critical parameter for photovoltaic applications.

### **First Graph: Effect of SILAR Cycles (100, 200, 300)**

- **Bandgap Narrowing:** As the number of SILAR cycles increases from 100 to 300, the bandgap of  $\text{Cu}_2\text{O}$  decreases. This is evident from the shift of the absorption edge towards lower energies (longer wavelengths) with increasing cycle number.
- **Explanation:** Increasing SILAR cycles leads to thicker films. In thicker films, there's a higher probability of defect formation and grain boundaries, which can introduce energy states within the bandgap, effectively narrowing it. Additionally, thicker films might experience strain or quantum confinement effects, further contributing to bandgap narrowing.

## Second Graph: Calcined vs. non-calcined

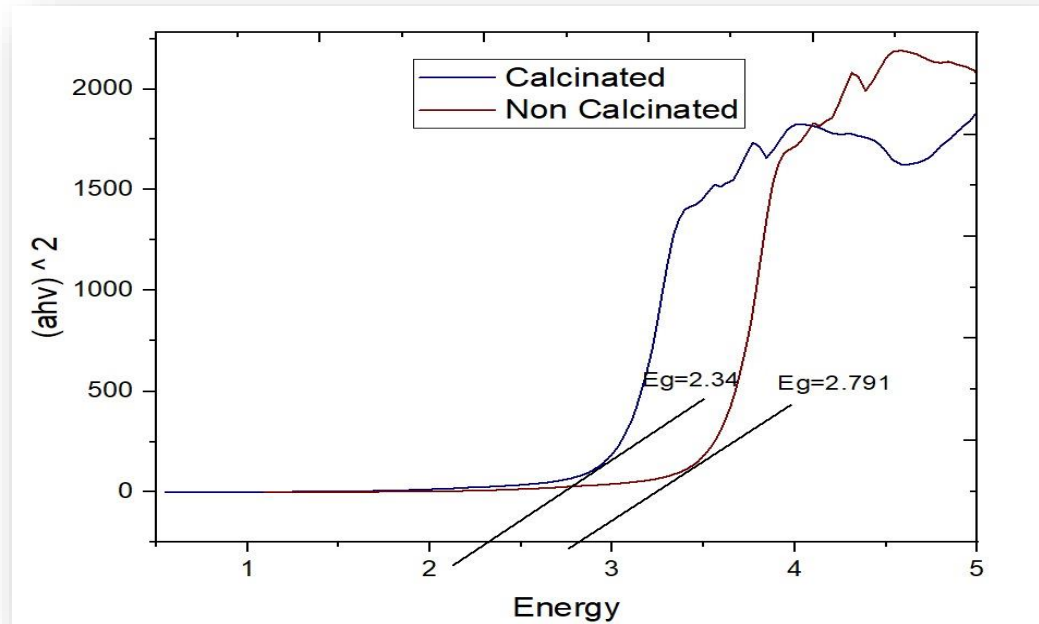


Figure 25 Tauc Plot showing Energy Gap values of Calcinated and Non-Calcinated Samples of Copper(I)Oxide

- **Bandgap Narrowing After Calcination:** The calcined  $\text{Cu}_2\text{O}$  film exhibits a narrower bandgap compared to the non-calcined film. This is indicated by the shift of the absorption edge towards lower energies after calcination.
- **Explanation:** Calcination improves the crystallinity of the  $\text{Cu}_2\text{O}$  film. A more ordered crystal structure results in fewer defects and a better-defined band structure, leading to a narrower bandgap.

## RAMAN Spectroscopy:

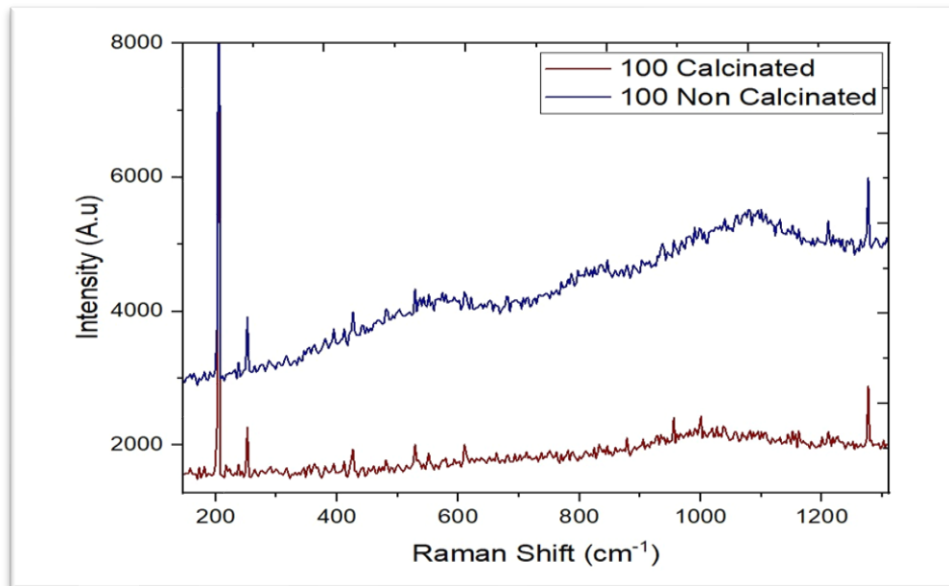
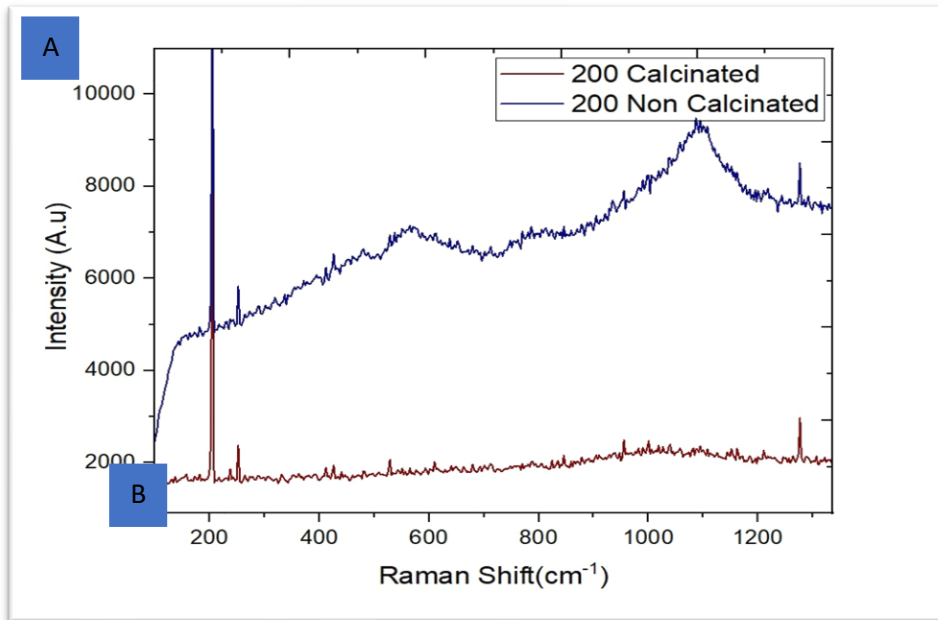


Figure 26 RAMAN Spectroscopy of Calcinated and Non-Calcinated Copper(I)Oxide at A)200 Cycles and B)100 Cycles

## **Explanation:**

The Raman spectra provide insights into the structural characteristics of copper(I) oxide ( $\text{Cu}_2\text{O}$ ) coatings on FTO glass, which are intended as p-type layers in all-oxide solar cells. Let's analyze each spectrum:

### **200 SILAR Cycles:**

- **Non-Calcined:** The spectrum shows a broad and poorly defined peak around  $520\text{ cm}^{-1}$ , which is characteristic of  $\text{Cu}_2\text{O}$ . However, the intensity is low, and the peak is broad, suggesting poor crystallinity and the presence of impurities or other copper oxide phases.
- **Calcined:** After calcination, the spectrum exhibits sharper and more intense peaks, particularly the prominent  $\text{Cu}_2\text{O}$  peak at  $520\text{ cm}^{-1}$ . This indicates a significant improvement in crystallinity and a reduction in impurities. The presence of additional peaks at lower wavenumbers (around  $220\text{ cm}^{-1}$  and  $300\text{ cm}^{-1}$ ) could be due to phonon modes associated with the improved crystal structure.

### **100 SILAR Cycles:**

- **Non-Calcined:** Similar to the 200-cycle non-calcined sample, this spectrum shows a weak and broad peak around  $520\text{ cm}^{-1}$ , indicating poor crystallinity and potential impurities.
- **Calcined:** Calcination again leads to a significant enhancement in crystallinity, as evidenced by the sharper and more intense  $\text{Cu}_2\text{O}$  peak at  $520\text{ cm}^{-1}$ . However, the overall peak intensity is lower than the 200-cycle calcined sample, suggesting that the 100-cycle film is thinner or less crystalline.

## SOLAR SIMULATION USING I-V CURVES

## 6.1 Light

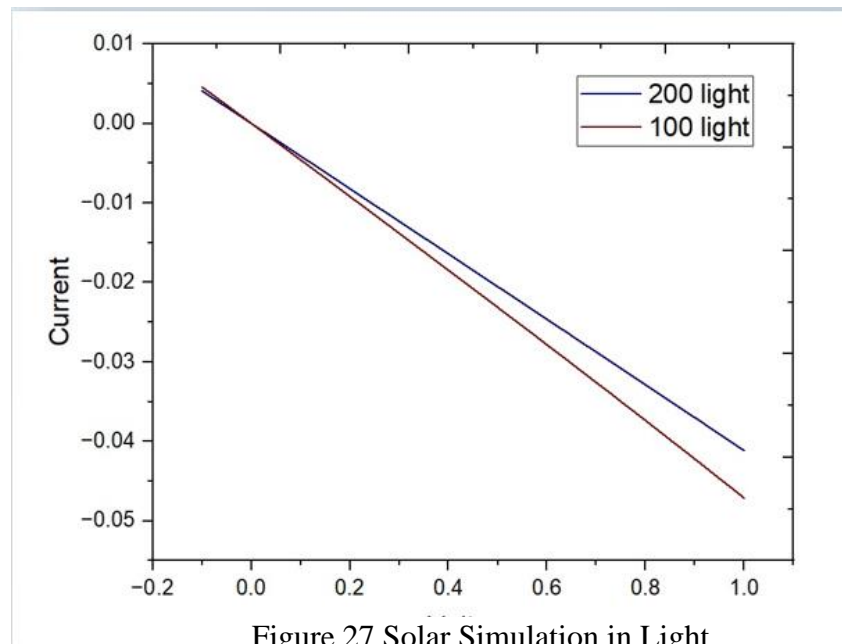


Figure 27 Solar Simulation in Light

**Explanation:**

The I-V curves you provided show the current-voltage characteristics of two solar cells under illumination, one with a 100 light intensity and the other with 200 light intensity. The curves exhibit several key features indicative of a short-circuited device due to the high evaporation rate during thermal evaporation:

1. **Lack of Characteristic Solar Cell Behavior:** Typical I-V curves for solar cells under illumination exhibit a distinct shape with a maximum power point (MPP), open-circuit voltage ( $V_{oc}$ ), and short-circuit current ( $I_{sc}$ ). In the provided curves, there is no clear MPP or  $V_{oc}$ , and the curves appear linear.

This lack of characteristic features suggests that the solar cell is not functioning properly.

- 2. Negative Current:** The current values in the graph are negative. This is an unusual behavior for a solar cell under illumination, where positive current flow is expected from the device. The negative current indicates a reverse current flow, which is a typical sign of a short-circuited device.
- 3. Linear Relationship:** The I-V curves exhibit a linear relationship between current and voltage, resembling a simple resistor's behavior. This is not expected for a solar cell, which should have a non-linear I-V relationship due to the diode-like behavior of the p-n junction.
- 4. Intensity Dependence:** The current values become more negative with increasing light intensity. This is consistent with a short-circuited device, where the magnitude of the reverse current is proportional to the number of light-generated carriers.

## 6.2 Dark

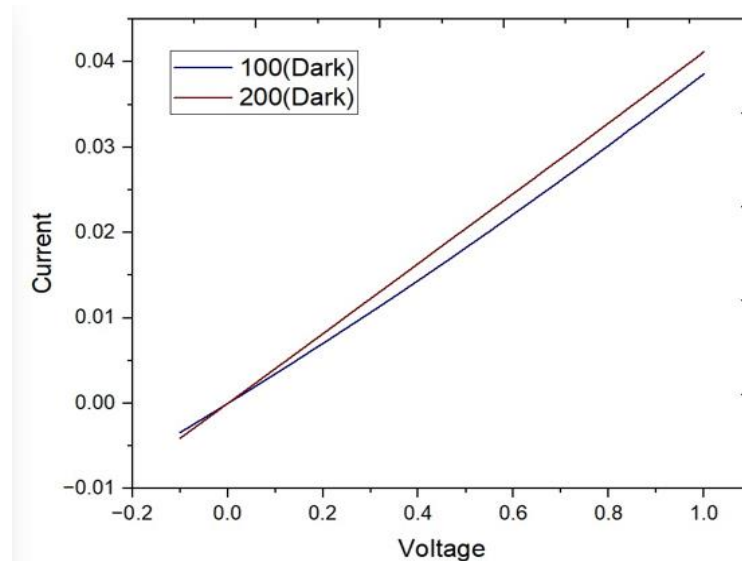


Figure 28 Solar Simulation in Dark

### Explanation:



The I-V curves in the dark for the short-circuited devices exhibit a linear relationship between current and voltage, with both 100 and 200 samples showing similar behavior. This linear relationship is indicative of ohmic conduction, suggesting that the short circuit is creating a dominant resistive path within the device.

**Here's a breakdown of the observations:**

- **Linearity:** The straight-line nature of the curves indicates a constant resistance, where the current is directly proportional to the applied voltage. This behavior is typical for simple resistors and is not expected for a functional solar cell, which should exhibit a diode-like characteristic in the dark.
- **Similar Slopes:** The 100 and 200 samples have nearly identical slopes, suggesting that the short-circuit resistance is not significantly affected by the difference in deposition cycles. This could imply that the short circuit is caused by a common factor, such as pinholes or other defects in the layers, rather than a difference in the thickness or quality of the Cu<sub>2</sub>O layer.
- **No Rectifying Behavior:** The absence of any rectifying behavior (non-linearity) in the curves further confirms the presence of a short circuit. A functional solar cell would show a much higher resistance in the reverse bias region, leading to a non-linear I-V curve.

## CHAPTER 7

### INTEGRATION OF AOSCs ON SMART WINDOW

The integration of Advanced Organic Solar Cells (AOSC) with smart windows offers a promising approach to creating sustainable buildings. Smart windows are electronically controlled windows that adjust their properties in response to external stimuli like sunlight and temperature, offering significant advantages for sustainable buildings. These features include reduced heat gain, improved daylight harvesting, and enhanced insulation.

AOSC technology presents a game-changer for smart windows, as it is thin, flexible, transparent, and lightweight. Two potential approaches for incorporating AOSC on smart windows are laminated AOSC Films and AOSC-integrated Smart Window Substrate. The integration of AOSC on smart windows offers several sustainability benefits, including energy generation, reduced building energy consumption, and lower carbon footprint.

However, challenges need to be addressed, such as AOSC efficiency, cost-effectiveness, and durability and longevity. Currently, AOSC efficiency is lower compared to traditional silicon solar cells, but research is ongoing to improve it for large-scale building applications. As AOSC technology matures, production costs are expected to decrease.

In conclusion, the integration of AOSC on smart windows holds immense potential for creating sustainable buildings by generating electricity, improving energy efficiency, and reducing reliance on fossil fuels. As AOSC research advances and cost considerations are addressed, widespread adoption of AOSC-powered smart windows in sustainable building design is expected.

## CONCLUSION

Using copper(I) oxide ( $\text{Cu}_2\text{O}$ ) for the p-type junction and titania ( $\text{TiO}_2$ ) for the n-type junction, we successfully created an all-oxide solar cell in our investigation. Utilizing the Successive Ionic Layer Adsorption and Reaction (SILAR) technique, the  $\text{Cu}_2\text{O}$  layer was deposited and optimised, guaranteeing a consistent and effective p-type semiconductor layer. The spin coating method was used to apply the n-type  $\text{TiO}_2$  layer, which produced a uniform and well-adhered layer required for ideal junction formation. The device structure was then completed by depositing a silver metal back contact using the thermal evaporation process.

But, a major problem arose during the fabrication process: the fast rate of evaporation of silver during thermal evaporation led to penetration through the layers, which resulted in short circuits in our devices. This demonstrated how crucial it is to have exact control over the deposition settings in order to shield the underlying semiconductor layers from harm.

In the future, we want to use machine learning algorithms to forecast and optimize our solar cells' I-V properties. Predictive models that incorporate process factors and experimental data allow us to simulate our devices' electrical performance in a variety of scenarios. In order to train and validate our models, this method will include gathering extensive data sets on voltage, current, ambient factors, and layer attributes.

We want to use a range of machine learning methods, including support vector regression, polynomial regression, decision trees, random forests, and neural networks. These models will aid in our comprehension of the intricate connections between material qualities, device performance, and production parameters. We can determine the ideal circumstances for maximizing our solar cells' current conversion efficiency by forecasting the I-V curves.

## 9. REFERENCES

1. Dimopoulos, T.J.T.f.o.s.o.i.n.-g.s.c., *All-oxide solar cells*. 2018: p. 439-480.
2. Scharber, M.C., et al., *Design rules for donors in bulk-heterojunction solar cells—Towards 10% energy-conversion efficiency*. 2006. **18**(6): p. 789-794.
3. Beiley, Z.M., et al., *Morphology-dependent trap formation in high performance polymer bulk heterojunction solar cells*. *Advanced Energy Materials*, 2011. **1**(5): p. 954-962.
4. Brabec, C.J., et al., *Origin of the open circuit voltage of plastic solar cells*. *Advanced Functional Materials*, 2001. **11**(5): p. 374-380.
5. Rafea, M.A. and N. Roushdy, *Determination of the optical band gap for amorphous and nanocrystalline copper oxide thin films prepared by SILAR technique*. *Journal of Physics D: Applied Physics*, 2008. **42**(1): p. 015413.
6. Parhizkar, M., et al., *Nanocrystalline CuO films prepared by pyrolysis of Cu-arachidate LB multilayers*. *Colloids and Surfaces A: Physicochemical and Engineering Aspects*, 2005. **257**: p. 277-282.
7. Mahalingam, T., et al., *Preparation and microstructural studies of electrodeposited Cu<sub>2</sub>O thin films*. *Materials letters*, 2004. **58**(11): p. 1802-1807.
8. Shiu, H.-Y., et al., *Solution-processed all-oxide nanostructures for heterojunction solar cells*. 2011. **21**(44): p. 17646-17650.
9. Shinagawa, T., et al., *Annealing effects and photoelectric properties of single-oriented Cu<sub>2</sub>O films electrodeposited on Au (111)/Si (100) substrates*. *Journal of Materials Chemistry A*, 2013. **1**(32): p. 9182-9188.
10. Nishi, Y., T. Miyata, and T. Minami, *The impact of heterojunction formation temperature on obtainable conversion efficiency in n-ZnO/p-Cu<sub>2</sub>O solar cells*. *Thin Solid Films*, 2013. **528**: p. 72-76.
11. Lakshmanan, A., Z.C. Alex, and S.J.M.T.S. Meher, *Recent advances in cuprous oxide thin film based photovoltaics*. 2022. **20**: p. 100244.
12. Green, M., et al., *Solar cell efficiency tables (version 57)*. *Progress in photovoltaics: research and applications*, 2021. **29**(1): p. 3-15.

13. Rao, M.K., et al., *Review on persistent challenges of perovskite solar cells' stability*. Solar Energy, 2021. **218**: p. 469-491.
14. Kaphle, A., et al., *Enhancement in the performance of nanostructured CuO-ZnO solar cells by band alignment*. RSC advances, 2020. **10**(13): p. 7839-7854.
15. Wijesundera, R., *Fabrication of the CuO/Cu<sub>2</sub>O heterojunction using an electrodeposition technique for solar cell applications*. Semiconductor science and technology, 2010. **25**(4): p. 045015.
16. Minami, T., T. Miyata, and Y. Nishi, *Relationship between the electrical properties of the n-oxide and p-Cu<sub>2</sub>O layers and the photovoltaic properties of Cu<sub>2</sub>O-based heterojunction solar cells*. Solar energy materials and solar cells, 2016. **147**: p. 85-93.
17. Olsen, L., F. Addis, and W. Miller, *Experimental and theoretical studies of Cu<sub>2</sub>O solar cells*. Solar cells, 1982. **7**(3): p. 247-279.
18. Iwanowski, R. and D. Trivich† dr, *Enhancement of the photovoltaic conversion efficiency in Cu/Cu<sub>2</sub>O schottky barrier solar cells by H<sup>+</sup> ion irradiation*. physica status solidi (a), 1986. **95**(2): p. 735-741.
19. Rai, B., *Cu<sub>2</sub>O solar cells: a review*. Solar cells, 1988. **25**(3): p. 265-272.
20. Rased, N., et al., *Introduction to solar energy and its conversion into electrical energy by using dye-sensitized solar cells*, in *Energy Materials*. 2021, Elsevier. p. 139-178.

## **APPENDIX**

### **What does the future hold?**

The integration of Advanced Organic Solar Cells (AOSC) with smart window technology is a promising path towards sustainable buildings. Technological advancements are expected to enhance AOSC efficiency, yield more transparent materials, and explore self-healing AOSC to address concerns about long-term durability and performance degradation. As AOSC research progresses, the technology is expected to become more readily available and cost-effective. Improved integration methods between AOSC and smart window technologies will likely emerge, optimizing aesthetics, functionality, and overall system efficiency. Government policies and incentives promoting sustainable building practices could accelerate the adoption of AOSC-integrated smart windows.

AOSC-integrated smart windows could find applications in vehicles, greenhouses, and mobile electronic devices. They could also be integrated with IoT sensors and controls, enabling intelligent building management systems that optimize energy use based on real-time data. A wider range of colors and transparency levels for AOSC could cater to diverse architectural design preferences. Challenges and considerations include environmental impact assessment, recycling and reusability strategies, and establishing industry standards and regulations for AOSC performance and integration with smart windows. However, the future of AOSC-integrated smart windows is bright, with ongoing research, cost reduction, and a growing focus on sustainability.

### **Integration of AOSCs on Perovskite solar cell**

The combination of Advanced Organic Solar Cells (AOSC) and perovskite solar cells for smart windows presents challenges due to efficiency trade-offs and transparency limitations. Perovskite solar cells are known for their high efficiency but stacking them with AOSC would likely introduce efficiency losses. Additionally, perovskite

cells can be efficient at absorbing light, which may not be ideal for achieving high transparency in a smart window application.

Alternative strategies for achieving high efficiency and transparency in smart windows include single-layer perovskite with improved transparency, and tandem perovskite-silicon cells. Research is ongoing to develop perovskite compositions designed for high transparency while maintaining good light absorption in desired wavelengths. AOSC can still play a role in smart window systems, such as powering control systems and building integrated photovoltaics (BIPV). A separate AOSC layer on the window could generate electricity to power the smart window's control system, reducing reliance on the building's grid. In conclusion, while AOSC and perovskite combination may seem like a perfect fit for smart windows, there are efficiency and transparency trade-offs to consider. Research into transparent perovskite compositions and tandem solar cell configurations holds more promise for achieving high efficiency and transparency in smart windows.